

# Can we Constrain Concept Bottleneck Models to Learn Semantically Meaningful Input Features?

Jack Furby<sup>1</sup>, Daniel Cunningham<sup>2,3</sup>, Dave Braines<sup>2</sup> and Alun Preece<sup>1</sup>

<sup>1</sup>Cardiff University

<sup>2</sup>IBM Research Europe

<sup>3</sup>Imperial College London  
furbyjl@cardiff.ac.uk

## Abstract

Concept Bottleneck Models (CBMs) are considered inherently interpretable because they first predict a set of human-defined concepts before using these concepts to predict the output of a downstream task. For inherent interpretability to be fully realised, and ensure trust in a model’s output, we need to guarantee concepts are predicted based on semantically mapped input features. For example, one might expect the pixels representing a broken bone in an image to be used for the prediction of a fracture. However, current literature indicates this is not the case, as concept predictions are often mapped to irrelevant input features. We hypothesise that this occurs when concept annotations are inaccurate or how input features should relate to concepts is unclear. In general, the effect of dataset labelling on concept representations in CBMs remains an understudied area. Therefore, in this paper, we examine how CBMs learn concepts from datasets with fine-grained concept annotations. We demonstrate that CBMs can learn concept representations with semantic mapping to input features by removing problematic concept correlations, such as two concepts always appearing together. To support our evaluation, we introduce a new synthetic image dataset based on a playing cards domain, which we hope will serve as a benchmark for future CBM research. For validation, we provide empirical evidence on a real-world dataset of chest X-rays, to demonstrate semantically meaningful concepts can be learned in real-world applications.

## 1 Introduction

Concept Bottleneck Models (CBMs) [Koh *et al.*, 2020] have been positioned as improving human collaboration as they are inherently interpretable [Koh *et al.*, 2020]. This capability is enabled by the model predicting a vector of human-defined concepts and a downstream task. Concept predictions can be inspected and modified to reveal the reasoning the model

made for a downstream task prediction. However, this may be misleading to humans interpreting the machine’s outputs if the model does not predict concepts based on their expected input features, but the human assumes it does. For humans to make full use of a model they will need to trust the model’s output but a lack of understanding of the causes for a decision will instead result in a loss of trust [Miller, 2019]. To benefit the most from CBM’s capabilities, they will need to be trained so input features map to concepts that align semantically.

During training both the concepts and downstream task are supervised with the model split into two parts, the input to the concept vector, the  $x \rightarrow c$  model part, and the concept vector to the downstream task, the  $c \rightarrow y$  model part. Splitting the model enables a human to intervene in the concept predictions by modifying them and passing them back through the  $c \rightarrow y$  model part [Koh *et al.*, 2020]. Let’s say we have a model diagnosing patients from X-ray images using concepts such as “fracture” or “edema”, a radiologist can add or remove concepts from the model outputs which may result in a vastly different downstream task output and thus may influence their overall decision-making. As CBMs do not reveal the input image features used for concept predictions, the radiologist’s decision, made in collaboration with the model, may assume the model is making use of the same features they used, potentially resulting in a diagnosis missing overlooked features or including irrelevant ones.

*Semantically meaningful* concept mapping is when concepts are predicted based on input features with the same meaning. For instance, if a CBM predicted the concept “fracture” we may expect the pixels representing the bone and break to be the primary input features used if the model has learned a Semantically meaningful concept mapping, and is not generally distributed over the entire subject in the input image. Current literature indicates CBMs do not map input features to concepts semantically [Furby *et al.*, 2023; Margeloiu *et al.*, 2021]. The authors use saliency maps produced with model-specific techniques, such as Integrated gradients (IG) [Sundararajan *et al.*, 2017] or Layer-wise Relevance Propagation (LRP) [Bach *et al.*, 2015], to visualise the relevance of input features. It is thought that CBMs are taking shortcuts [Furby *et al.*, 2023] or encoding other information in the concept vector [Marconato *et al.*, 2022; Espinosa Zarlenga *et al.*, 2023]. It is possible, however, that this could be caused by CBMs being trained on inaccurate

or weakly defined concept annotations. A popular dataset for CBM research is a modified version of Caltech-UCSD Birds-200-2011 (CUB) [Wah *et al.*, 2011] with class-level concepts [Koh *et al.*, 2020], where each sample in a class has the same set of concepts. Most concepts for CUB represent parts of a bird, however, if the image is cropped, or the bird changes appearance with gender or age, concepts may no longer match the visual appearance in the image. As CBMs are only trained on task and concept labels they have no ground truth as to what features they should use from dataset samples and instead are left to discover this. If concepts are not carefully considered when designing a dataset then there could be concepts that always appear together, potentially causing unintentional concept correlations, concepts that only appear for one downstream task, opening a shortcut the model may use for downstream task prediction, or concepts that do not have a visual representation in the input. We hypothesise that using a dataset with accurate and well-defined concepts, a CBM can learn concept representations with semantic mappings from input features. To the best of our knowledge, the dataset has had little consideration for how it affects concept representations with the only research into semantic concept mapping using the previously mentioned CUB dataset [Furby *et al.*, 2023; Margeloiu *et al.*, 2021].

This paper presents a comprehensive analysis of the concept representations CBMs learn with various dataset configurations. We focus on training CBMs on images containing visual features that represent concepts. Our datasets include a synthetic image dataset, which enables us to explore a best-case scenario, and a chest X-ray image dataset, which demonstrates a real-world use case. Our contributions are threefold; (1) In contrast to previous studies, we demonstrate the ability of CBMs to learn concept representations that hold semantic mapping to the input space. This was shown by (2) introducing a new synthetic image dataset with fine-grained concept annotations. (3) We performed an in-depth analysis of CBMs and concluded that two factors are critical for CBMs to learn semantically meaningful input features: (i) accuracy of concept annotations and (ii) high variability in the combinations of concepts co-occurring.

## 2 Related Work

Previous work has explored the mappings CBMs learn [Furby *et al.*, 2023; Margeloiu *et al.*, 2021]. These show that CBMs fail to map concept outputs to semantically meaningful areas in the input image, however, they only focus on class-level concepts with the dataset CUB. This dataset has concept annotations representing visual attributes of birds but, birds can look different when they are young and old or male and female, and some concepts may be hidden from view. This was highlighted by [Furby *et al.*, 2023] and could explain the inability of CBMs to learn a semantically meaningful mapping to input features. To the best of our knowledge, there is no prior work which looks at the attribution of relevance to the input features that contribute to a model’s output(s) with CBMs trained on datasets with instance-level concepts, where each sample in a dataset has its own concept vector [Koh *et*

*al.*, 2020], or datasets with accurate concept annotations and where the correlation between concepts has been carefully considered. Instance-level concept annotations avoid the inaccurate concept annotations seen with CUB as concepts can be fine-grained, only setting concepts to present when their visual representations can be identified in the input. We cannot jump to the conclusion that instance-level concepts are all you need. The original CUB dataset [Wah *et al.*, 2011] has instance-level concepts, but these were noisy [Koh *et al.*, 2020] which may restrict the model learning semantically meaningful concept mappings.

Other metrics to analyse the concepts CBMs learn fall under the term *concept leakage* [Mahinpei *et al.*, 2021], and originate from *disentanglement* metrics [Bengio *et al.*, 2013], where it’s generally desired for concepts to only encode information than is required to predict themselves. [Mahinpei *et al.*, 2021] evaluates whether concepts excluded from training can be predicted better than a random guess, while [Marconato *et al.*, 2022] trains models on fixed data ranges and tests whether concepts can be predicted outside of these constraints. [Espinosa Zarlenga *et al.*, 2023] introduces Oracle and Niche scores to measure *concept purity*. These scores measure inter-concept predictability w.r.t. the expected predictive performance of the dataset. Concept purity is argued to be better suited to CBMs than existing disentanglement metrics.

We position our work for smaller and specialised tasks [Oikarinen *et al.*, 2023] due to the complexity of creating large-scale datasets with concept annotations [Kazhdan *et al.*, 2021]. Moving beyond this, recent developments with Large Language Models [Oikarinen *et al.*, 2023; Yang *et al.*, 2023] and language-vision model, CLIP [Radford *et al.*, 2021], have the potential to automate the annotation process. Large Language Models are used to generate potential concepts and CLIP discards concepts not relevant to the input image. For now, however, we cannot guarantee all generated concepts relate to semantically meaningful input features in the input image. This can be observed in [Oikarinen *et al.*, 2023] with the concept “junk” for an image of a car or “long tail with white stripes” for an image of a bird where the tail is obscured in the image.

## 3 Concept Bottleneck Models

A CBM takes an input, in our case an image, which is passed through the  $x \rightarrow c$  model part, predicting a vector of concepts. Concept predictions are then passed through the  $c \rightarrow y$  model part to predict a downstream task. Concept predictions are in the range of 0 to 1 where 0 means the model is confident the concept is not present and a prediction of 1 means the model is confident the concept is present. Predictions of 0.5 and above are counted as present. A CBM prediction can be intervened by adjusting the concept outputs with new values within the range 0 and 1 and then performing the forward pass with the new set of concepts and the  $c \rightarrow y$  model part to get a new downstream task prediction.

CBMs are trained by supervising both the concepts and the downstream task given the training set  $\{x^{(i)}, y^{(i)}, c^{(i)}\}_{i=1}^n$  where we are provided with a set of inputs  $x \in \mathbb{R}^d$ , corre-

sponding targets  $y \in \mathcal{Y}$  and vectors of  $k$  concepts  $c \in \mathbb{R}^k$ . A CBM in the form  $f(g(x))$  uses two functions:  $g : \mathbb{R}^d \rightarrow \mathbb{R}^k$  to map an input to the concept space, and  $f : \mathbb{R}^k \rightarrow \mathcal{Y}$  to map concepts to the downstream task output. This is such that the downstream task prediction is made using only the predicted concepts.

There are three methods we can train a CBM; the *independent* method where each model part is trained separately and then joined together after training, the *sequential* method where the model parts are trained one after another, or the *joint* methods where the model parts are trained together.

In this paper we also train CBMs with training sets  $\{x^{(i)}, c^{(i)}\}_{i=1}^n$  and  $\{y^{(i)}, c^{(i)}\}_{i=1}^n$  and thus can train the model part for function  $g$  on a separate dataset to the model part for function  $f$ . The only limitation this causes is we are unable to train models using the joint method. This should not be a concern as the training method does not appear to make a difference to model accuracy [Marconato *et al.*, 2022].

## 4 Experiment Set-up

We address if CBMs can learn to map semantically meaningful input features to concepts and the effect inter-concept predictability of a dataset has on learned concept representations. For each of our experiments, we have the following dataset and model set-up.

### 4.1 Datasets

We train our models on two datasets: Playing cards, a new synthetic image dataset to evaluate CBMs with perfect concept annotations, and CheXpert, a real-world X-ray image dataset.

**Playing cards:** Playing cards is a synthetic image dataset we’re introducing to analyse CBMs free of noise and with control over how clear input features map to concept labels. Playing cards is comprised of 40,000 images in four variations: (1) single playing card, (2) three random playing cards, referred to as *random cards*, (3) three playing cards with a downstream task of classifying hand ranks in the game Three Card Poker, referred to as *poker cards*, a smaller and faster-paced version of the card game Poker, and (4) a version of poker cards with a reduced set of concepts, referred to as *class-level poker cards*. Each variation has a 70%-30% split between training and validation images. Both random cards and poker cards have instance-level concepts where the concepts represent the playing cards present in the input images. Class-level poker cards use class-level concepts with 11 concepts instead of the full 52 from random and poker cards. In all cases, if a concept is annotated as present, then it is visible in the corresponding image. The dataset is available for download<sup>1</sup>.

**CheXpert [Irvin *et al.*, 2019]:** We use CheXpert as an example of a real-world image dataset with visually represented concepts. We use 13 signs for the concepts with the attribute “no\_findings” as the downstream task. CheXpert has instance-level concepts. The dataset contains 224,316 chest X-ray images that were scaled to 512 x 512 pixels. We use

<sup>1</sup>Playing cards dataset: Available for camera-ready submission

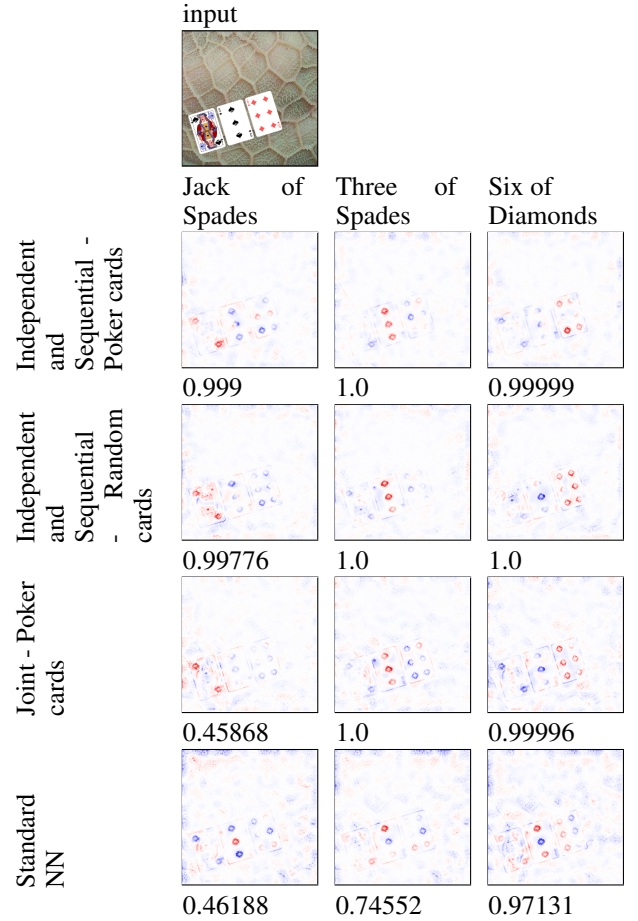


Figure 1: Positive relevance (red) is always applied to the expected input features (playing cards) when concept supervision is used in training.

the official dataset splits from [Irvin *et al.*, 2019]. For validating the model we only use frontal-view images, 202 in total. The dataset was configured with U-ones annotations which set any missing values to 0 and any uncertain annotations to 1. We also modify CheXpert to use class-level concepts with the most common concept vector for three, four and five concepts present. We refer to the original version of CheXpert as *instance-level CheXpert* and the class-level modifications as *class-level CheXpert*.

### 4.2 Models

The playing cards models use a VGG-11 architecture with batch normalisation [Simonyan and Zisserman, 2015] for the  $x \rightarrow c$  model part. For the  $c \rightarrow y$  model part, we use two linear layers with a ReLU activation function. Between the two model parts, we use a sigmoid function as this increases the independence of concept representations than the logits alternative [Espinosa Zarlenga *et al.*, 2023]. We evaluate these models w.r.t. the combined concept and downstream task loss. Our random cards models achieve an average concept accuracy of 99.932%, poker card models have an average concept accuracy of 99.914% and class-level poker cards

have an average concept accuracy of 99.99%. To compare CBM with a standard Neural Network (NN) we also trained models on poker cards but without concept loss, achieving an average concept accuracy of 50.25%.

Our CheXpert models use a Densenet121 architecture [Huang *et al.*, 2017] for the  $x \rightarrow c$  model part and pre-trained weights from ImageNet and two linear layers with a ReLU activation function for the  $c \rightarrow y$  model part. We evaluate this model w.r.t. Area Under the receiver operating characteristic Curve (AUC), following previous work [Ye *et al.*, 2020; Chauhan *et al.*, 2023]. Our instance-level CheXpert models achieve an average concept accuracy of 76.82% while class-level CheXpert models archived an average concept accuracy of 57.127%, 61.418% and 60.962% for the dataset version with three, four and five concepts present respectively.

Full details on model training and performance for playing card models and CheXpert models can be found in the Appendix A.1.

## 5 Experiments and Results

In this section, we analyse our models using both qualitative and quantitative metrics. Where relevant we have provided additional samples in the Appendix B.

### 5.1 Input Feature Importance

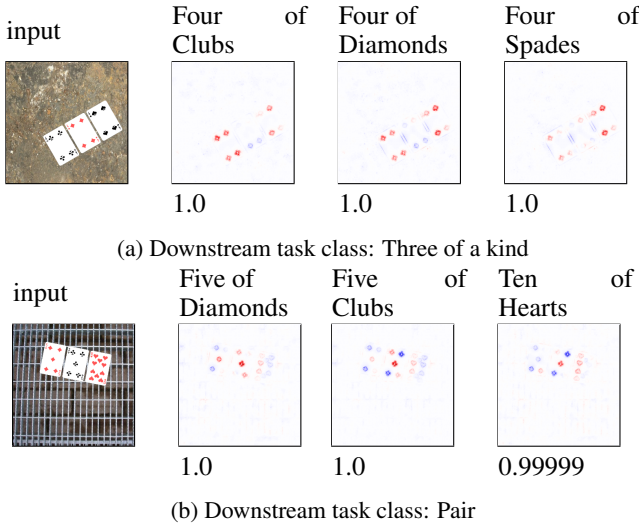


Figure 2: Despite accurate concept predictions, positive saliency (red) does not always map to the semantic input features for each concept.

We first evaluate feature importance using saliency mapping techniques with the playing card models. We use model-specific methods which utilise the model architecture to produce explanations by propagating a gradient backwards through the model [Bach *et al.*, 2015; Sundararajan *et al.*, 2017; Selvaraju *et al.*, 2017]. Each of the explanation techniques produces saliency maps where we display positive relevance in red and negative relevance in blue. Saliency maps are local explanations which means any explanation only relates to a single sample and model. We are therefore limited

to using these to highlight biases in the model [Ribeiro *et al.*, 2016] or otherwise provide a qualitative evaluation of feature importance.

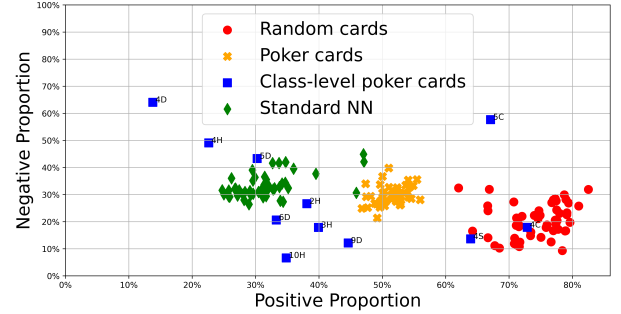


Figure 3: Random cards and poker cards both have a high positive proportion of relevance, indicating the models have learned a semantic mapping to concepts, unlike standard NN and most concepts for class-level poker cards.

We use the technique LRP to explain the playing card models with the rules [Bach *et al.*, 2015]  $LRP-\alpha\beta$ , where  $\alpha = 1$  and  $\beta = 0$ , for the first four convolutional layers of the model from the input,  $LRP-\epsilon$  for the next four convolutional layers and  $LRP-0$  for the top three linear layers. These rules were selected to be similar to those used by [Montavon *et al.*, 2019].

Figure 1 shows for random and poker card CBMs the most positively salient input features are symbols on the playing cards. Positive saliency is primarily contained to the corresponding playing card for each concept with negative relevance distributed over the other playing cards. As we do not specify which input features the model should use for each concept, and we can see the models have selected features within semantically meaningful playing cards, we consider these reasonable input features for the model to use. Our standard NN was unable to localise relevance to the semantically meaningful playing cards and instead distributed it over all three cards present. In Figure 2 we show saliency maps for models trained with class-level poker cards. Despite class-level concepts being used by [Furby *et al.*, 2023; Margeloiu *et al.*, 2021], using our dataset we successfully trained our models to recognise concepts with a semantic mapping from input features to concepts. However, this is limited to just a few concepts (see Four of Clubs and Four of Spades in Figure 2a). In total, only 3 concepts consistently have positive relevance applied to them by the model. This was to be expected as for some concepts there is more ambiguity regarding which input features the model should use. Class-level poker cards was designed so some concepts have a clear input feature to concept mapping such as in Figure 2a, the concepts used for the downstream task class Three of a kind are also used by other downstream classes, while others do not, such as in Figure 2b, Five of Clubs is only used for the downstream task class Pair. Other concepts are confined to appearing in pairs or threes.

To analyse if our playing card models are applying relevance to semantically meaningful input features with a quantitative metric, we can measure the proportion of relevance

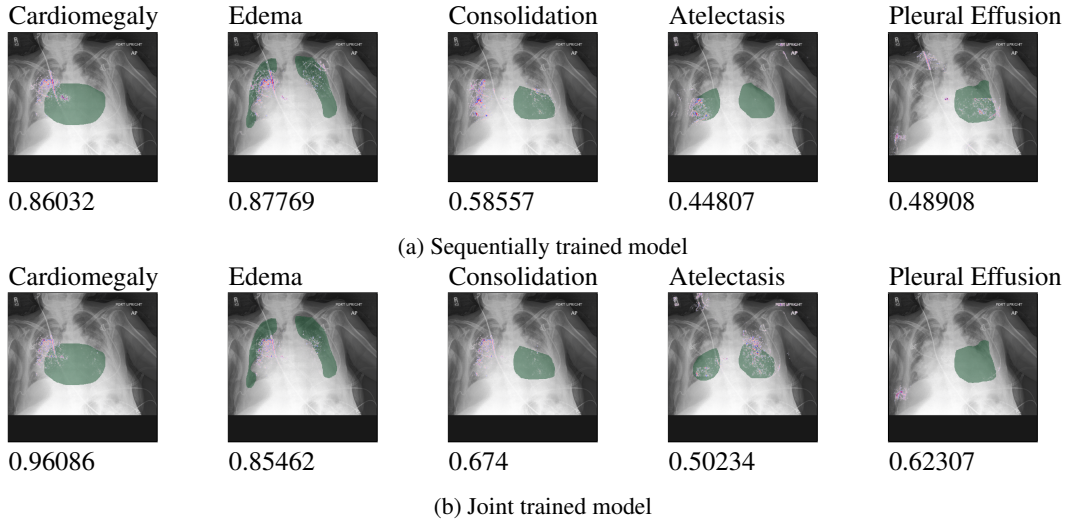


Figure 4: Concept saliency maps for chest X-rays with instance-level CheXpert shows reasonable localisation of concepts to ground truth areas of the input image.

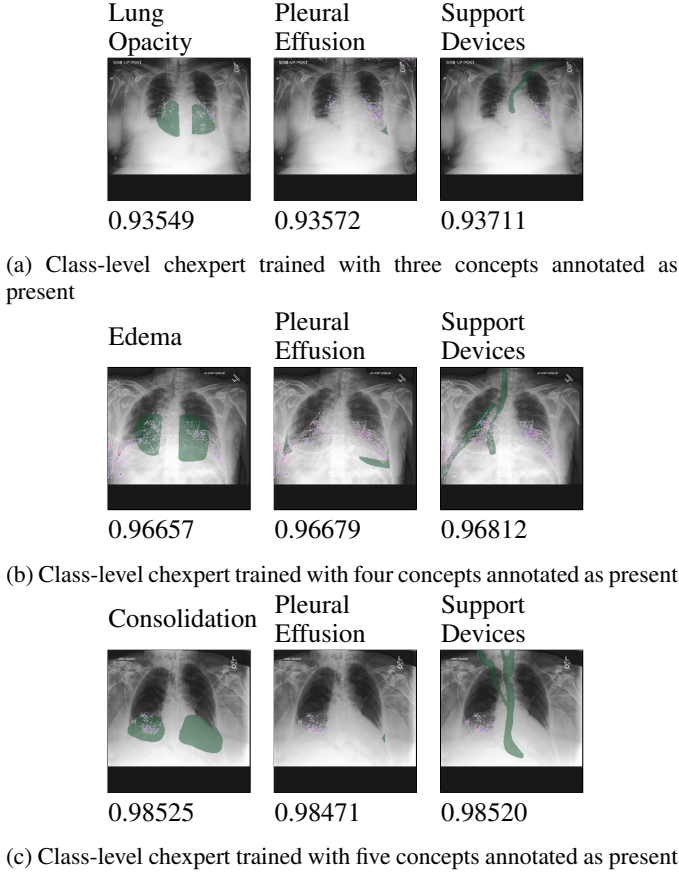


Figure 5: Concept saliency maps for class-level CheXpert shows the model is using similar input features to predict all present concepts

applied to concepts' visual representations. If the proportion of positive relevance is high, and the proportion of negative relevance is low, then we can argue the model has learned a

semantically meaningful concept mapping. We compare our random cards, poker cards, class-level poker cards, and standard NN models in Figure 3 with averaged proportions over 5 models for each dataset variant. Each point represents a single concept. Relevance on the background is discarded as it plays no part in predicting concepts. The plot shows three distinct clusters, one for each of random cards, poker cards and the standard NN. Random cards have the highest proportion of positive relevance and the lowest proportion of negative relevance. Poker cards have less positive relevance and more negative relevance but still show an improvement from the standard NN. Combining this plot with the saliency maps we saw in Figure 1 confirms the CBMs have learned to apply relevance to semantically meaningful input features for both random cards and poker cards, although less so for poker cards. As random cards have concepts selected at random, whereas poker cards concepts are restricted to what the downstream task permits (e.g. Straight Flush requires three cards of the same suit and incriminating values), this plot shows how a reduction of concept correlation benefits CBMs learning semantic concept mappings. In this case, caused by the downstream task. The points for class-level poker cards are not clustered together. Most concepts have a low proportion of relevance, meaning a semantically meaningful concept mapping has not been learned. A few concepts however, Four of Spades, Four of Clubs and Five of Clubs have a high proportion of positive relevance. For the concepts Four of Spades and Four of Clubs, this confirms what we saw in Figure 2a, that a semantically meaningful concept mapping has been learned. The same cannot be said for the concept Five of Clubs as all saliency maps for concepts predicted as present when this concept is in the input image, apply positive relevancy to this concept's semantic input features (see Figure 2b), inflating the positive proportion we see. Class-level poker cards reveal the challenge of engineering a dataset with enough constraints for the model to learn semantically meaningful concept mappings. Even though the concepts Four of

Spades and Four of Clubs show it possible for a CBM to learn semantically meaningful concept mappings with class-level concepts, the consistency in relevancy proportions with random cards and poker cards shows the advantage instance-level concepts can provide.

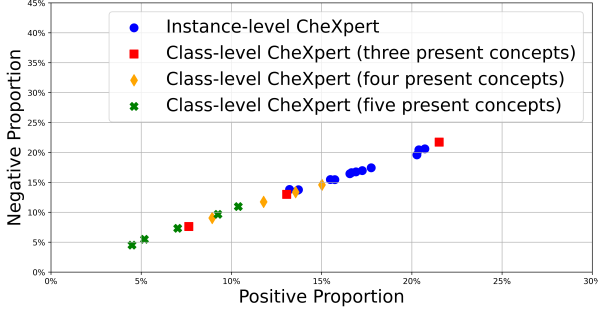


Figure 6: Instance-level CheXpert has more positive relevancy attributed to ground truth segmentations than class-level CheXpert for most concepts.

To evaluate CBM’s ability to map semantic input features to concepts in a real-world setting we have trained CBMs on the dataset CheXpert. As the dataset domain is on chest X-rays, most images will contain the relevant input features to map to concept annotations. Essentially as all concepts represent visual signs in the chest region, and all images are chest X-rays, then concepts should have a visual representation in the corresponding input image. As uncertain or missing concepts are set to present, there will be some noise in the training data and we may assume there is some additional noise caused by the annotations originally being generated using an automated labeller [Irvin *et al.*, 2019]. For our results in Figure 4, we are using the saliency mapping technique Guided Grad-CAM [Selvaraju *et al.*, 2017] and our models trained on instance-level CheXpert. To validate that the models have mapped concepts to intended input features we are using ground truth segmentations from [Saporta *et al.*, 2022]. These were created by two board-certified radiologists and ensure our conclusions are made w.r.t. expert opinion. Our results show concepts trained on instance-level CheXpert can map concepts to semantic input features for both models trained with the independent/sequential method 4a and joint method 4b. The concepts for Edema, Consolidation, Atelectasis and Pleural effusion all should be observable with signs in the lungs while Cardiomegaly is observed by an enlarged heart and thus should either highlight the heart or areas around the heart. From the samples we show, most concepts map to features within the ground truth segmentation such as the saliency maps for the concepts Atelectasis and Edema. The saliency maps for the concept Consolidation maps to the incorrect lung which may be considered a reasonable error to make, the model is still mapping to the correct organ. As for the concept Cardiomegaly, the model still maps to the lungs, but most relevance is outside of the ground truth segmentation. Instance-level CheXpert saliency maps are distinctly different to each other and do not appear to be using the same input features for every concept prediction, unlike

class-level CheXpert as we see in Figure 5 where all concept saliency maps highlight similar input features irrespective of the concept being predicted.

The proportion of relevance using our joint trained CheXpert models is shown in Figure 6. The maximum positive saliency is much lower than playing cards, topping out just over 20% and the concepts for instance-level CheXpert are not clustered but instead form a line. As discussed by [Saporta *et al.*, 2022], the most accurate concepts tend to be larger in size which could explain this. We are however more interested in the differences between instance-level CheXpert and class-level CheXpert. Instance-level CheXpert generally outperforms class-level CheXpert at mapping input features to concept segmentations. Most class-level concepts have a very little positive proportion of relevance located to the ground truth segmentations. We can therefore take away the concept annotations for instance-level CheXpert can confine models to learn semantic input features and further reinforces the need to avoid training CBMs on concepts that are only present together.

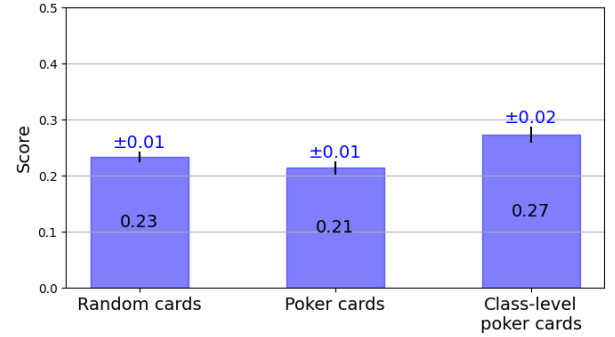
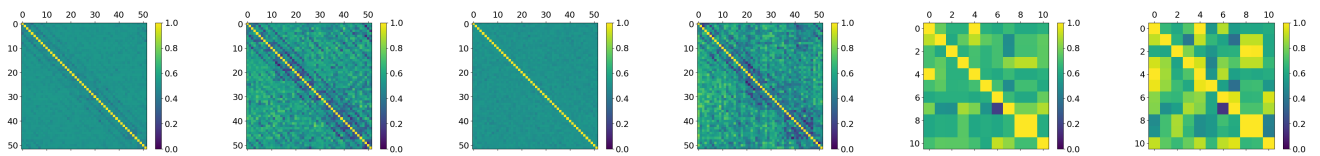


Figure 7: OIS is a metric for measuring additional or lacking information in learned concepts. This plot shows averaged OIS values for random cards, poker cards and class-level poker cards. Random and poker cards show high concept purity as the OIS value is close to 0 while class-level has a lower concept purity.

## 5.2 Concept Purity

If we can train CBMs to learn semantically meaningful input features we may also expect an improvement in concept purity. We measure concept purity using the Oracle Impurity Score (OIS) [Espinosa Zarlenga *et al.*, 2023]. Our configuration uses a helper model formed of a two-layer ReLU multi-layer perceptron with 32 activations in its hidden layer. Concept representation quality is defined as purity, whether a learned concept representation has a predictive power similar to what would be expected from ground truth labels. OIS is the divergence of two matrices; the predictability of ground truth concepts w.r.t. one another, the oracle matrix, and the predictability of ground truth concepts from learned concepts, the purity matrix. If OIS results in a value of 0 then learned concepts do not encode any more or less information than is required to predict themselves whereas a value of 1 means each learned concept can predict all other concepts.

OIS results for poker cards, random cards (both tested with the poker cards dataset), and class-level poker cards are



(a) Poker cards oracle matrix (b) Poker cards purity matrix (c) Random cards oracle matrix (d) Random cards purity matrix (e) Class-level poker cards oracle matrix (f) Class-level poker cards purity matrix

Figure 8: Oracle and purity matrices for random cards, poker cards and class-level poker cards. The oracle matrices show inter-concept predictability of ground truth concepts while the purity matrices show inter-concept predictability of learned concepts w.r.t. ground truth concepts. Poker cards show numerous diagonals of non-random concept predictability. class-level poker cards show a high level of inter-concept predictability exist within learned concept representations.

shown in Figure 7. We cannot use OIS with our CheXpert models as OIS makes use of AUC. As the test dataset split for CheXpert has a limited number of samples, a few concepts have one or zero annotations representing the concepts as being present. Results for playing cards are averaged over 5 training runs using the independent  $x \rightarrow c$  training method with each set of weights used to generate an OIS value 3 times. Models trained on poker cards show a marginal improvement over random cards with class-level poker cards having the highest OIS value. These results may appear unexpected given how random cards should have no inter-concept predictability, unlike poker cards and class-level poker cards. OIS however is w.r.t. the expected impurities that exist in the dataset. If a number of ground truth concepts have a high correlation and the concept representations have the same correlation then the OIS metric will show low impurity. If however the concept representations capture different correlations then the OIS metric will show higher impurities.

To expand on the OIS scores we have visualised the two matrices from the OIS value for each dataset variation, shown in Figure 8. Each coordinate in these matrices shows the predictability for one concept predicting another concept as an AUC value. All oracle matrices show a strong predictability for each concept predicting itself, which is to be expected. The oracle matrix for Figure 8a shows additional diagonals with AUC values lower than 0.5, where concepts in the dataset have information for non-random inter-concept predictability. These diagonals are not present in the random concepts dataset, Figure 8c. Looking at the purity matrices for playing cards, Figure 8b and Figure 8d, the additional diagonals of inter-concept predictability continues for poker cards but there is a distinct reduction with random cards. Remembering the OIS value can either show extra information or a lack of information w.r.t. the expectation from the dataset, the higher value for random cards in Figure 7 is likely showing a lack of expected information. For class-level poker cards the oracle matrix, Figure 8e, shows mostly random inter-concept predictability apart from for a few concepts. These concepts are those that are only used for a single downstream task. The purity matrices have many more concepts with increased inter-concept predictability although they are all located to concepts within a few steps from the concepts with non-random inter-concept predictability in Figure 8e. This shows the models have encoded extra information for each concept than is required, for instance,

the concepts Six or Nine of Diamonds (index 8 and 9) are only present when the Four of Diamonds (index 3) is present. Therefore the concepts Six or Nine will never be present if the Four of Clubs (index 2) is present.

## 6 Discussion and Conclusion

In this paper, we realise the original promise of CBM’s inherent interpretability by training models which map concepts to semantically meaningful input features. This benefits inherent interpretability as we can be sure the model is predicting concepts for the right reasons, and not due to some unintended dataset configuration. If a CBM makes predictions using semantically mapped input features, we can argue the model will be easier to build trust with as concept predictions will use the expected input features from a human perspective. We achieved semantically meaningful concept mappings by training CBMs with accurate concept annotations and with a high variety of concepts that are present together. This differs from the previously analysed CUB dataset with class-level concepts which cannot account for visual changes in the input images. The semantically meaningful concept mappings do not come from the use of class or instance-level concepts, but instead from ensuring if a concept is annotated as present in the dataset then it is visually present in the corresponding image and the occurrence of concepts in the dataset do not create unintended correlations. We however demonstrate it’s easier to achieve semantically meaningful concept mappings with instance-level concept annotations.

We show how learned concept representations can encode correlations between concepts from the dataset which may lead to concepts being predicted based on the presence or absence of other concepts. If this is to be avoided the correlation of concepts in the dataset should be considered, and if the downstream task restricts this, can be avoided by splitting the training of the two model parts to learn concepts and the downstream task separately.

Future research regarding the representations CBMs learn should focus on CBMs trained on larger datasets. Although [Oikarinen *et al.*, 2023] shows how large language models and CLIP can be used to train an iteration of CBMs, removing the need for manual concept annotations, the semantic mapping from concepts to input features remains unclear. Ensuring concept annotations have a semantic mapping, even for large or machine-generated datasets, or including another

constraint to achieve semantically meaningful concept mappings, should be a priority for ensuring inherent interpretability and human trust can be achieved.

## References

- [Bach *et al.*, 2015] Sebastian Bach, Alexander Binder, Grégoire Montavon, Frederick Klauschen, Klaus-Robert Müller, and Wojciech Samek. On pixel-wise explanations for non-linear classifier decisions by layer-wise relevance propagation. *PLOS ONE*, 10(7):1–46, 07 2015.
- [Bengio *et al.*, 2013] Y. Bengio, Aaron Courville, and Pascal Vincent. Representation learning: A review and new perspectives. *IEEE transactions on pattern analysis and machine intelligence*, 35:1798–1828, 08 2013.
- [Biewald, 2020] Lukas Biewald. Experiment tracking with weights and biases, 2020. Software available from wandb.com.
- [Chauhan *et al.*, 2023] Kushal Chauhan, Rishabh Tiwari, Jan Freyberg, Pradeep Shenoy, and Krishnamurthy Dvijotham. Interactive concept bottleneck models. *Proceedings of the AAAI Conference on Artificial Intelligence*, 37(5):5948–5955, Jun. 2023.
- [Espinosa Zarlenga *et al.*, 2023] Mateo Espinosa Zarlenga, Pietro Barbiero, Zohreh Shams, Dmitry Kazhdan, Umang Bhatt, Adrian Weller, and Mateja Jamnik. Towards robust metrics for concept representation evaluation. *Proceedings of the AAAI Conference on Artificial Intelligence*, 37(10):11791–11799, Jun. 2023.
- [Furby *et al.*, 2023] Jack Furby, Daniel Cunningham, Dave Braines, and Alun Preece. Towards a deeper understanding of concept bottleneck models through end-to-end explanation. *R2HCAI: The AAAI 2023 Workshop on Representation Learning for Responsible Human-Centric AI*, 2023.
- [Huang *et al.*, 2017] Gao Huang, Zhuang Liu, Laurens van der Maaten, and Kilian Q. Weinberger. Densely connected convolutional networks. In *Proceedings of the IEEE Conference on Computer Vision and Pattern Recognition (CVPR)*, July 2017.
- [Irvin *et al.*, 2019] Jeremy Irvin, Pranav Rajpurkar, Michael Ko, Yifan Yu, Silviana Ciurea-Ilcus, Chris Chute, Henrik Marklund, Behzad Haghighi, Robyn Ball, Katie Shpankaya, Jayne Seekins, David A. Mong, Safwan S. Halabi, Jesse K. Sandberg, Ricky Jones, David B. Larson, Curtis P. Langlotz, Bhavik N. Patel, Matthew P. Lungren, and Andrew Y. Ng. Chexpert: A large chest radiograph dataset with uncertainty labels and expert comparison. *Proceedings of the AAAI Conference on Artificial Intelligence*, 33(01):590–597, Jul. 2019.
- [Kazhdan *et al.*, 2021] Dmitry Kazhdan, Boty Dimanov, Helena Andres Terre, Mateja Jamnik, Pietro Liò, and Adrian Weller. Is disentanglement all you need? comparing concept-based & disentanglement approaches. *RAI workshop at The Ninth International Conference on Learning Representations 2021*, 2021.
- [Kingma and Ba, 2014] Diederik Kingma and Jimmy Ba. Adam: A method for stochastic optimization. *International Conference on Learning Representations*, 12 2014.
- [Koh *et al.*, 2020] Pang Wei Koh, Thao Nguyen, Yew Siang Tang, Stephen Mussmann, Emma Pierson, Been Kim, and Percy Liang. Concept bottleneck models. In Hal Daumé III and Aarti Singh, editors, *Proceedings of the 37th International Conference on Machine Learning*, volume 119 of *Proceedings of Machine Learning Research*, pages 5338–5348. PMLR, 13–18 Jul 2020.
- [Mahinpei *et al.*, 2021] A. Mahinpei, J. Clark, I. Lage, F. Doshi-Velez, and P. WeiWei. Promises and pitfalls of black-box concept learning models. In *proceeding at the International Conference on Machine Learning: Workshop on Theoretic Foundation, Criticism, and Application Trend of Explainable AI*, volume 1, pages 1–13, 2021.
- [Marconato *et al.*, 2022] Emanuele Marconato, Andrea Passerini, and Stefano Teso. Glancenets: Interpretable, leak-proof concept-based models, 05 2022.
- [Margeloiu *et al.*, 2021] Andrei Margeloiu, Matthew Ashman, Umang Bhatt, Yanzhi Chen, Mateja Jamnik, and Adrian Weller. Do concept bottleneck models learn as intended? *ICLR 2021 Workshop on Responsible AI*, 2021.
- [Miller, 2019] Tim Miller. Explanation in artificial intelligence: Insights from the social sciences. *Artificial Intelligence*, 267:1–38, 2019.
- [Montavon *et al.*, 2019] Grégoire Montavon, Alexander Binder, Sebastian Lapuschkin, Wojciech Samek, and Klaus-Robert Müller. *Layer-Wise Relevance Propagation: An Overview*, pages 193–209. Springer International Publishing, 09 2019.
- [Oikarinen *et al.*, 2023] Tuomas Oikarinen, Subhro Das, Lam M. Nguyen, and Tsui-Wei Weng. Label-free concept bottleneck models. In *The Eleventh International Conference on Learning Representations*, 2023.
- [Radford *et al.*, 2021] Alec Radford, Jong Wook Kim, Chris Hallacy, Aditya Ramesh, Gabriel Goh, Sandhini Agarwal, Girish Sastry, Amanda Askell, Pamela Mishkin, Jack Clark, Gretchen Krueger, and Ilya Sutskever. Learning transferable visual models from natural language supervision. In *International Conference on Machine Learning*, 2021.
- [Ribeiro *et al.*, 2016] Marco Ribeiro, Sameer Singh, and Carlos Guestrin. “why should I trust you?”: Explaining the predictions of any classifier. In *Proceedings of the 2016 Conference of the North American Chapter of the Association for Computational Linguistics: Demonstrations*, pages 97–101, San Diego, California, June 2016. Association for Computational Linguistics.
- [Saporta *et al.*, 2022] Adriel Saporta, Xiaotong Gui, Ashwin Agrawal, Anuj Pareek, Steven Q. H. Truong, Chanh D. T. Nguyen, Van-Doan Ngo, Jayne Seekins, Francis G. Blankenberg, Andrew Y. Ng, Matthew P. Lungren, and Pranav Rajpurkar. Benchmarking saliency methods for chest x-ray interpretation. *Nature Machine Intelligence*, 4, 2022.

- [Selvaraju *et al.*, 2017] Ramprasaath R. Selvaraju, Michael Cogswell, Abhishek Das, Ramakrishna Vedantam, Devi Parikh, and Dhruv Batra. Grad-cam: Visual explanations from deep networks via gradient-based localization. In *2017 IEEE International Conference on Computer Vision (ICCV)*, pages 618–626, 2017.
- [Simonyan and Zisserman, 2015] Karen Simonyan and Andrew Zisserman. Very deep convolutional networks for large-scale image recognition. In *International Conference on Learning Representations*, 2015.
- [Sundararajan *et al.*, 2017] Mukund Sundararajan, Ankur Taly, and Qiqi Yan. Axiomatic attribution for deep networks. In *Proceedings of the 34th International Conference on Machine Learning - Volume 70, ICML’17*, page 3319–3328. JMLR.org, 2017.
- [Wah *et al.*, 2011] C. Wah, S. Branson, P. Welinder, P. Perona, and S. Belongie. The Caltech-UCSD Birds-200-2011 Dataset. Technical Report CNS-TR-2011-001, California Institute of Technology, 2011.
- [Yang *et al.*, 2023] Yue Yang, Artemis Panagopoulou, Shenghao Zhou, Daniel Jin, Chris Callison-Burch, and Mark Yatskar. Language in a bottle: Language model guided concept bottlenecks for interpretable image classification. In *Proceedings of the IEEE/CVF Conference on Computer Vision and Pattern Recognition (CVPR)*, pages 19187–19197, June 2023.
- [Ye *et al.*, 2020] Wenwu Ye, Jin Yao, Hui Xue, and Yi Li. Weakly supervised lesion localization with probabilistic-cam pooling, 2020.

## A Experiments set-up

In this section, we provide further details on datasets, model architectures and training methods used in this paper. All experiments were run on a workstation with a single 24GB NVIDIA Quadro RTX 6000 GPU, Intel(R) Core(TM) i9-10900K CPU @ 3.70GHz and 64GB of system memory. The machine runs Ubuntu 22.04.3 LTS. We estimate around 500 hours are required to train models and run all experiments, which includes training each model 5 times on random seeds. All random seeds were selected using the shuf command to select a number between 0 and 1000.

### A.1 Models and training

**Playing cards:** All playing card models use a VGG-11 architecture with batch normalisation [Simonyan and Zisserman, 2015] for the  $x \rightarrow c$  model part. The  $c \rightarrow y$  model part used two linear layers with a ReLU activation function. Between the two model parts, we used a sigmoid function. During training, we evaluate these models w.r.t. the combined concept and downstream loss. We detail average model accuracies in Table 1. For experiments that used a single model (e.g. saliency map generation), we selected the model with the highest concept accuracy. These are detailed in Table 2.

We used Weights and Biases Sweeps [Biewald, 2020] to find optimal hyperparameters for training each of our models on the playing cards dataset. This was configured with a Bayesian search method to optimise the parameters. These were; starting learning rate (between 0.1 and 0.001), optimizer (between Adam [Kingma and Ba, 2014] and stochastic gradient descent (SGD)), learning rate patience (between 3, 5, 10 and 15 epochs of no improvement in loss) and theta value (A value used with joint training to balance concept and downstream task loss). Sweeps were run for each of the dataset variants and CBM training. Each sweep ran until we stopped seeing improvements in the model accuracy, about 30 iterations per sweep. The final hyperparameters we used are in Table 3.

**CheXpert [Irvin *et al.*, 2019]:** Our CheXpert models use a Densenet121 architecture [Huang *et al.*, 2017] for the  $x \rightarrow c$  model part and pre-trained weights, trained on Imagenet. The  $c \rightarrow y$  model part used two linear layers with a ReLU activation function. Between the two model parts, we used a sigmoid function. We evaluated these models w.r.t. Area Under the receiver operating characteristic Curve (AUC) for concepts. Averaged model performance is shown in Table 4. The best model accuracies are shown in Table 5 and AUC values in Table 6. These models were selected as they had the highest AUC values. Model training hyperparameters are listed in Table 7. We do not display AUC values for the concept ‘Fracture’ as there are no positive samples for this concept in the test dataset split.

### A.2 Datasets

**Playing cards:** Playing cards is a synthetic dataset where each sample has either one or three playing cards placed on a random background. Each sample has annotations for a downstream task classification, a series of concepts, and playing card coordinates. Playing cards are placed in a random

location on the background image, with a random size and rotation, but with the constraint that each playing card is fully visible. If three cards are in a sample, then they are placed in a line. We include four versions of the dataset; single playing card which includes one playing card and class-level concepts representing the suit and rank of the card, random cards which have three random playing cards, poker cards which have three playing cards that are selected based on a hand rank in the game Three Card Poker, and class-level poker cards which is similar to poker cards but has a reduced set of concepts. Random cards and poker cards have instance-level concepts with concepts representing cards present in each sample. Each variation has 10,000 samples where 70% are training images and 30% are testing/validation images. Example images are shown in Figure 9. Code to generate the dataset is publicly available<sup>2</sup>. The concepts in class-level poker cards represent playing cards but instead of 52 concepts, class-level poker cards reduce this to 11 concepts. These concepts are arranged such that some concepts are only used for one downstream task class while others are used for many. The mapping between concepts which appear in the same images is shown in Figure 10.

In this paper, we transform training samples with a random flip, both horizontal and vertical, apply a colour jitter to the brightness, contrast, saturation and hue, and randomly convert to grey scale. Samples are scaled to 299 by 299 pixels.

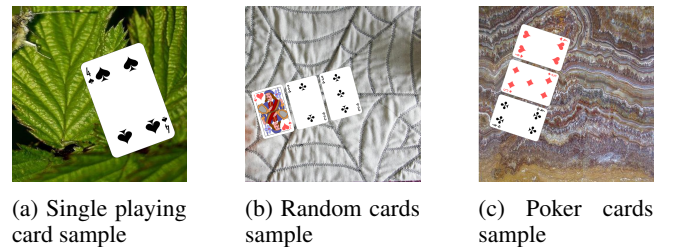


Figure 9: Samples from the Playing cards dataset

**CheXpert [Irvin *et al.*, 2019]:** CheXpert is an image dataset in the domain of chest X-rays. It has 14 signs, of which we have used 13 for concepts with the 14 (No findings) as the downstream task. The dataset contains 224,316 X-ray images. We use the official dataset splits from [Irvin *et al.*, 2019]. The original validation split was used as a holdout test split with only frontal-view images kept, 202 in total. We have configured the dataset to use U-ones annotations which sets any missing or uncertain annotations to 1 representing the sign as being present. For all samples in the training set, CheXpert used an automated annotator to label the 14 annotations from radiology reports. The test set was annotated by the consensus of 5 board-certified radiologists. During training, samples are randomly rotated by up to 15 degrees, translated by up to 5% of the overall image width and scaled by up to 5%. All samples are resized to 512 by 512 pixels.

<sup>2</sup>Playing cards dataset generator: Available in camera-ready submission

Training method	Dataset	Average concept accuracy (%)	Concept standard deviation	Average task accuracy (%)	Task standard deviation
Independent	Random cards	99.943	0.008	99.174	0.09
Sequential	Random cards	99.921	0.044	97.457	0.76
Independent	Poker cards	99.957	0.005	99.421	0.034
Sequential	Poker cards	99.917	0.051	98.802	0.277
Joint	Poker cards	99.867	0.046	96.005	0.213
Independent	Class-level poker cards	99.98	0.014	99.96	0.039
Sequential	Class-level poker cards	99.98	0.014	99.953	0.045
Joint	Class-level poker cards	100	0	100	0
Standard NN	Poker cards	50.25	1.31	67.137	0.584

Table 1: Playing card models averaged metrics. All values are rounded to 3 decimal places.

Model	Dataset	Concept accuracy (%)
Independent & Sequential	Random cards	99.961
Independent & Sequential	Poker cards	99.961
Independent & Sequential	Class-level poker cards	99.997
Joint	Poker cards	99.936
Standard NN	Poker cards	52.717

Table 2: Concept accuracy for models used to generate saliency maps

Training method & Dataset	Learning rate	Optimizer	Batch size	Learning patience	rate	Theta	Epochs
Independent & sequential $x \rightarrow c$ - Random cards	0.03	SGD	32	15		N/A	200
Independent & sequential $x \rightarrow c$ - Poker cards	0.02	SGD	32	15		N/A	200
Independent & sequential $x \rightarrow c$ - Class-level poker cards	0.0825	SGD	32	3		N/A	100
Independent $c \rightarrow y$ - Random cards	0.01	Adam	32	5		N/A	200
Independent $c \rightarrow y$ - Poker cards	0.01	Adam	32	5		N/A	200
Independent $c \rightarrow y$ - Class-level poker cards	0.064	Adam	32	5		N/A	100
Sequential $c \rightarrow y$ - Random cards	0.059	Adam	32	5		N/A	200
Sequential $c \rightarrow y$ - Poker cards	0.046	Adam	32	15		N/A	200
Sequential $c \rightarrow y$ - Class-level poker cards	0.0846	Adam	32	10		N/A	100
Joint - Poker cards	0.025	SGD	32	15		0.98	300
Joint - Class-level poker cards	0.0398	SGD	32	15		0.867	100
Standard NN - Poker cards	0.088	SGD	32	15		0	300

Table 3: Playing cards training hyperparameters

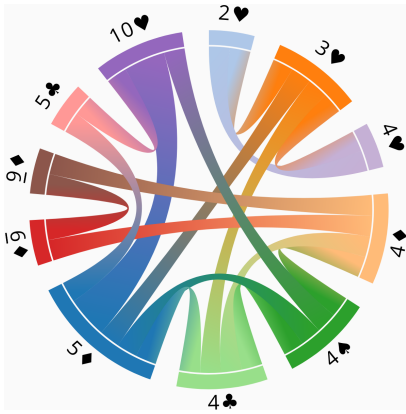


Figure 10: Class-level poker cards has concepts arranged such that some only appear in the same image with two other concepts (e.g. Two of Hearts, Three of Hearts and Four of Hearts) while some appear in the same image as many other concepts (e.g. Five of Diamonds)

## B Experiments and results

### B.1 Playing cards

We show additional concept saliency map results for our instance-level playing card models in Figure 11 and 12, 13, and 14. We provide examples of all downstream task classes for class-level poker card saliency maps to variations between all concept predictions. These can be seen in Figure 15, 16, 17, 18, 19 and 20. We used three explanation techniques; LRP, IG with a smoothgrad noise tunnel, and IG with a smoothgrad squared noise tunnel. For LRP we used the rules  $LRP-\alpha\beta$ , where  $\alpha = 1$  and  $\beta = 0$ , for the first four convolutional layers of the model from the input,  $LRP-\epsilon$  for the next four convolutional layers and  $LRP-0$  for the top three linear layers. IG with a smoothgrad noise tunnel is configured to use 25 randomly generated samples and a standard deviation of 0. Most saliency maps focus on the playing card that maps semantically to its corresponding concept. All saliency maps generated with LRP show positive relevancy attributed to the correct playing card for each concept to satisfy semantically meaningful feature mapping, while both IG variations show good localisation. IG with a smoothgrad squared noise tunnel applies little relevance in general and highlights a different card for the concept King of Hears in Figure 13.

### B.2 CheXpert

We show additional saliency maps results for instance-level CheXpert in Figure 21, 22, 23 and 24 using three explanation techniques; IG with a smoothgrad noise tunnel, and IG with a smoothgrad squared noise tunnel and GradCAM [Selvaraju *et al.*, 2017]. IG with a smoothgrad noise tunnel and IG with a smoothgrad squared noise tunnel is configured to use 25 randomly generated samples and a standard deviation of 0.2. For the most part, relevance is localised but fairly noisy, especially for IG. For a number of concepts, saliency is also not within ground truth segmentations (the areas highlighted with green). Each saliency map is distinctly different from concept to concept so we can tell the model is not using the same input features to predict each concept. Class-level CheXpert

in Figure 25, 26, 27, 28, 29 and 30 tell a different story as all concepts share very similar saliency maps and thus, the model is using the same input features to predict all concepts.

Training method	Dataset version	Concept accuracy (%)	Concept standard deviation	Task accuracy (%)	Task standard deviation
Sequential	Instance-level	75.971	1.77	0.865	0.001
Joint	Instance-level	77.659	1.578	0.883	0.009
Sequential	Class-level with 3 present concepts	58.044	9.141	62.414	0.023
Sequential	Class-level with 4 present concepts	62.268	10.004	36	0.014
Sequential	Class-level with 5 present concepts	61.971	6.754	36.571	0.021
Joint	Class-level with 3 present concepts	56.211	2.098	95.517	0.008
Joint	Class-level with 4 present concepts	60.569	8.727	95.429	0.034
Joint	Class-level with 5 present concepts	59.952	3.932	0.967	0.032

Table 4: CheXpert models averaged metrics. All values are rounded to 3 decimal places.

Model	Dataset version	Concept accuracy (%)
Sequential	Instance-level CheXpert	75.659
Joint	Instance-level CheXpert	78.668
Sequential	Class-level CheXpert with 3 present concepts	71.598
Sequential	Class-level CheXpert with 4 present concepts	68.71
Sequential	Class-level CheXpert with 5 present concepts	64.623

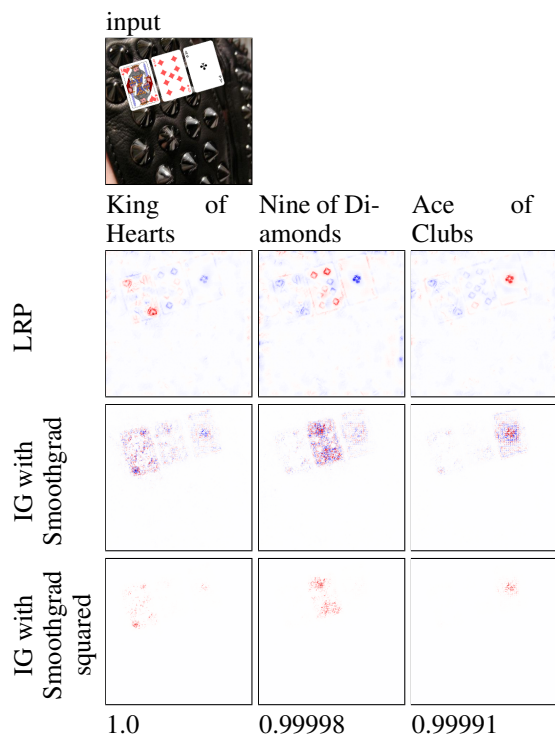
Table 5: Concept accuracy for models used to generate saliency maps

Concept	Sequential instance-level CheXpert	Joint instance-level CheXpert	Joint class-Level CheXpert with 3 present concepts	Joint class-Level CheXpert with 4 present concepts	Joint class-Level CheXpert with 5 present concepts
Enlarged cardiomeastium	0.525	0.547	N/A	N/A	N/A
Cardiomegaly	0.831	0.879	N/A	N/A	N/A
Lung opacity	0.933	0.912	0.998	1.0	1.0
Lung lesion	0.127	0.138	N/A	N/A	N/A
Edema	0.932	0.954	N/A	1.0	N/A
Consolidation	0.867	0.847	N/A	N/A	0.875
Pneumonia	0.572	0.628	N/A	N/A	N/A
Atelectasis	0.795	0.776	N/A	N/A	1.0
Pneumothorax	0.795	0.795	N/A	N/A	N/A
Pleural effusion	0.930	0.931	0.998	1.0	1.0
Plaural other	0.142	0.143	N/A	N/A	N/A
Support devices	0.966	0.959	0.998	1.0	1.0

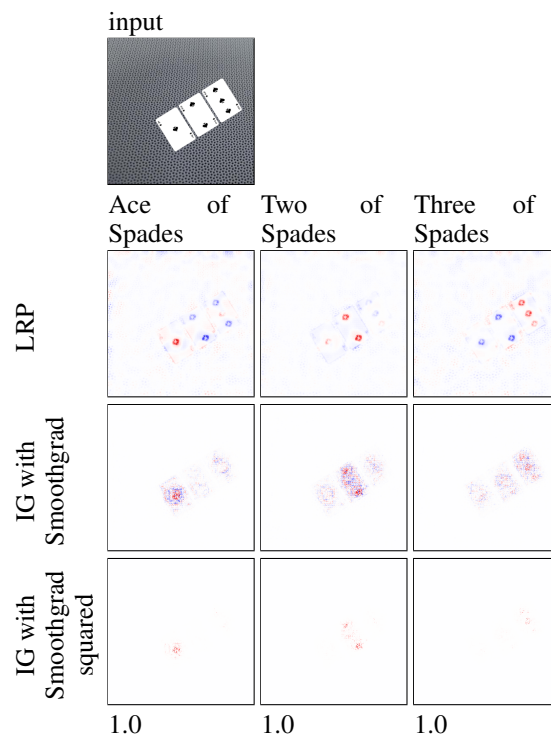
Table 6: Concept AUC for models used to generate saliency maps

Training method	Learning rate	Optimizer	Batch size	Learning rate patience	Theta	Epochs
Independent & sequential $x \rightarrow c$	0.0001	Adam	14	0.1	N/A	3
Sequential $c \rightarrow y$	0.0001	Adam	14	0.1	N/A	3
Joint	0.0001	Adam	14	0.1	0.99	3

Table 7: CheXpert training hyperparameters

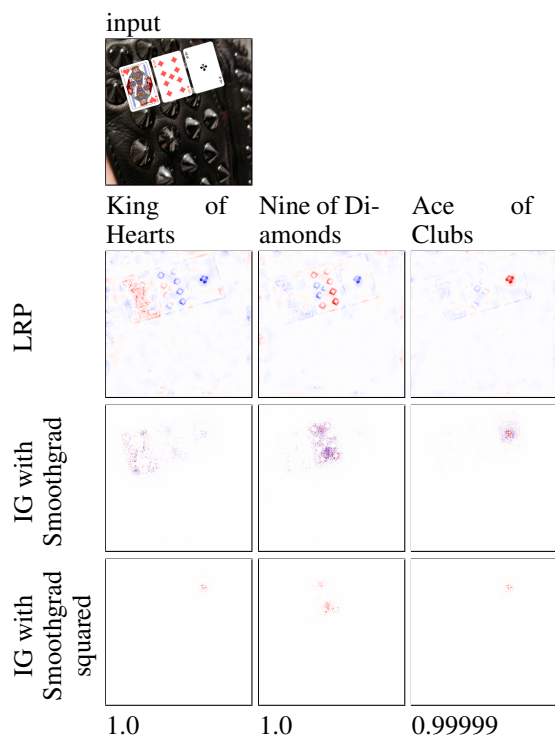


(a) High card downstream task classification

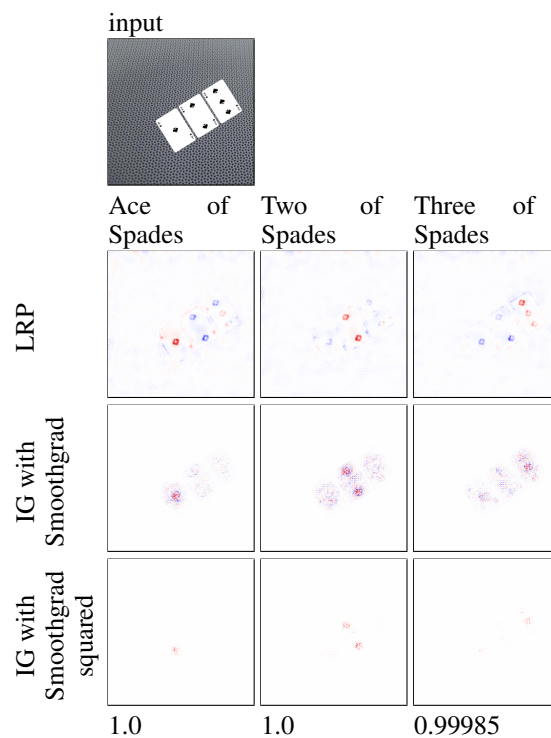


(b) Straight flush downstream task classification

Figure 11: Independent / sequential model trained on poker cards

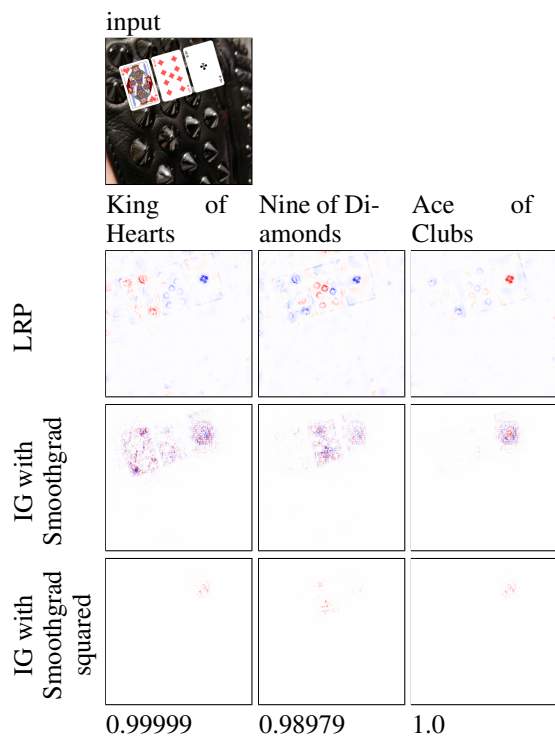


(a) High card downstream task classification high card

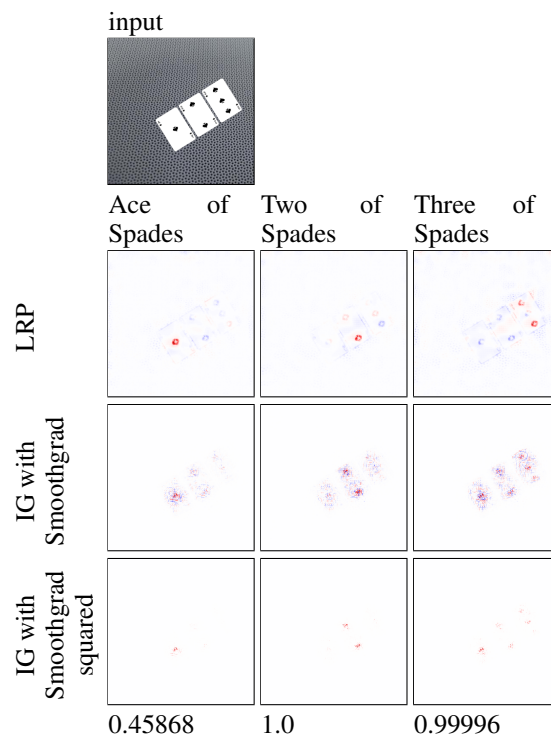


(b) Straight flush downstream task classification

Figure 12: Independent / sequential model trained on random cards

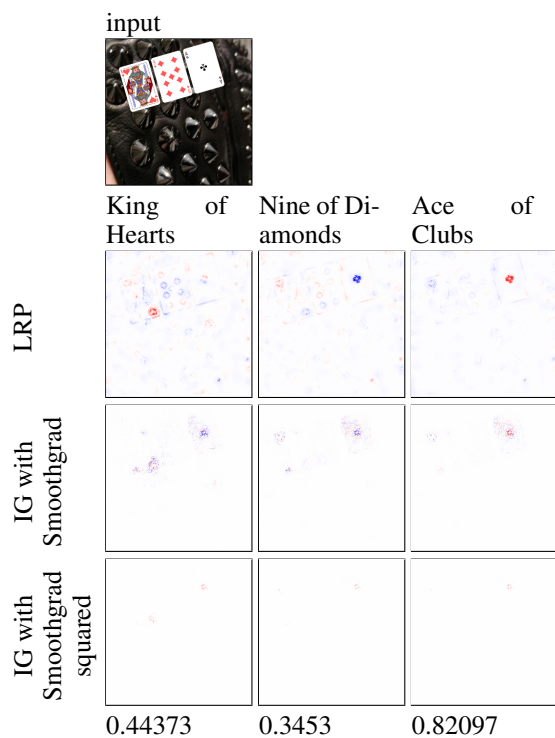


(a) High card downstream task classification

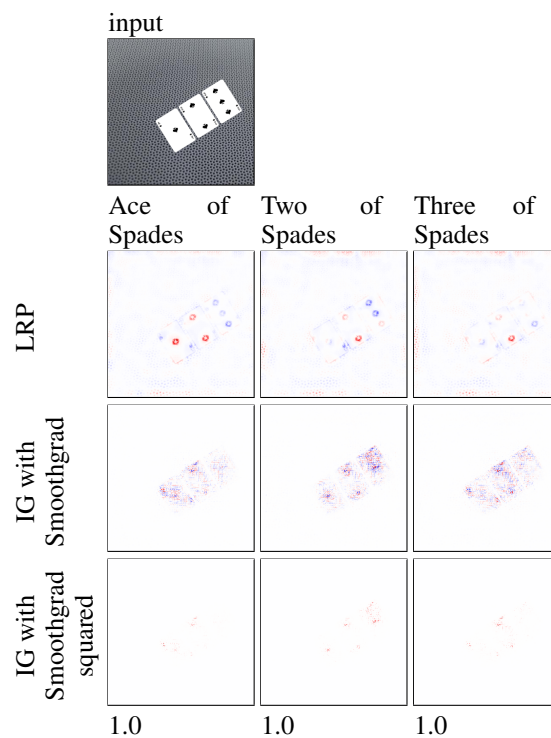


(b) Straight flush downstream task classification

Figure 13: Joint model trained on poker cards



(a) High card downstream task classification



(b) Straight flush downstream task classification

Figure 14: Standard NN model trained on poker cards

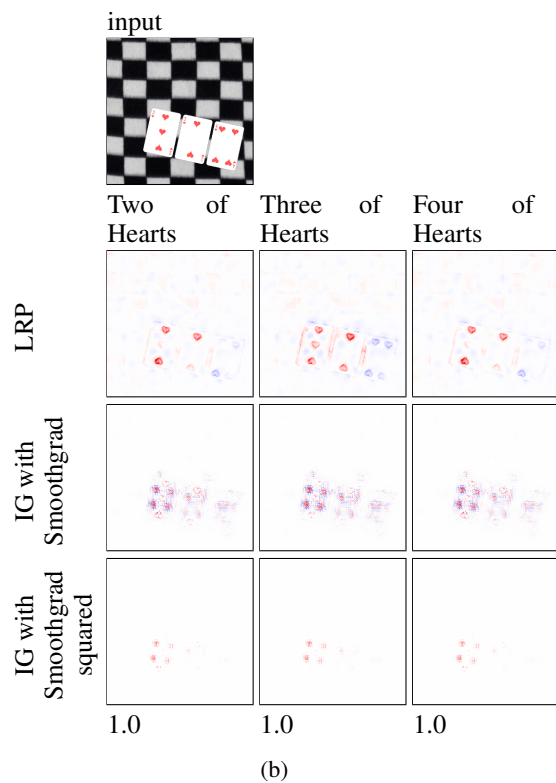
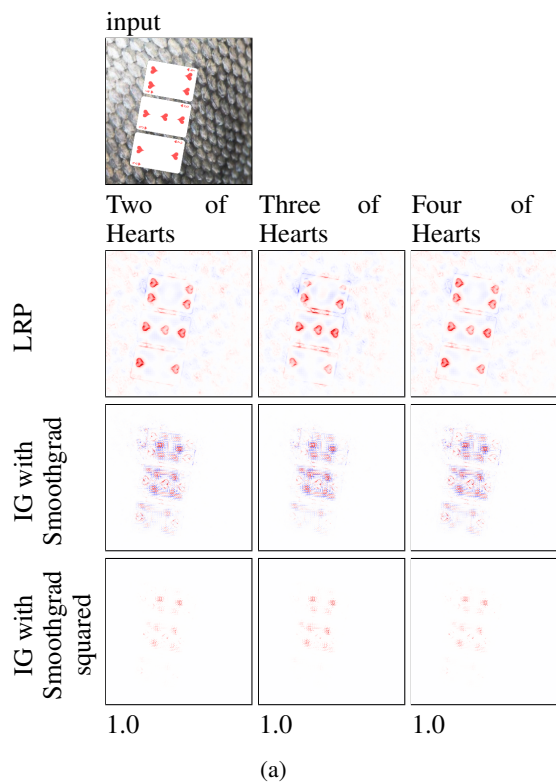


Figure 15: Class-level poker cards predicting concepts with the downstream task classification of Straight flush

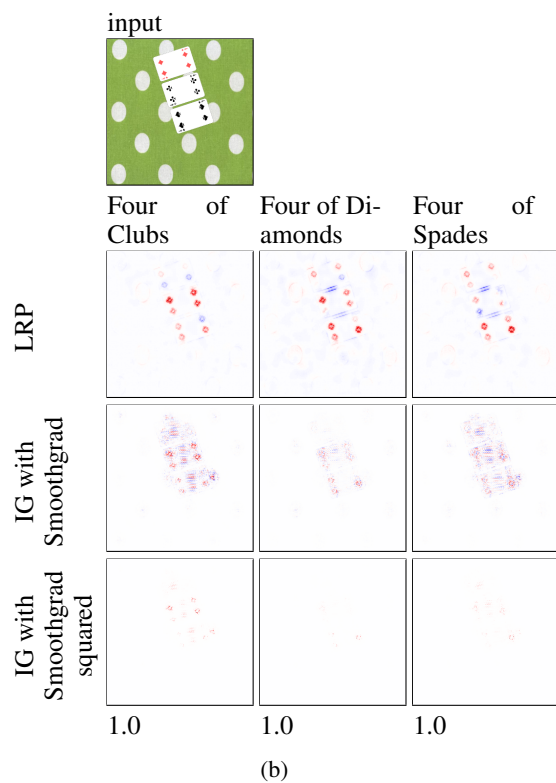
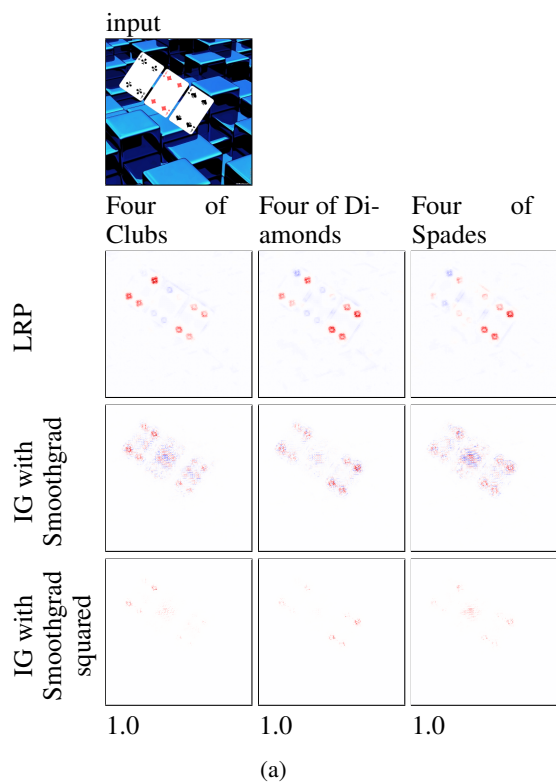


Figure 16: Class-level poker cards predicting concepts with the downstream task classification of Three of a kind

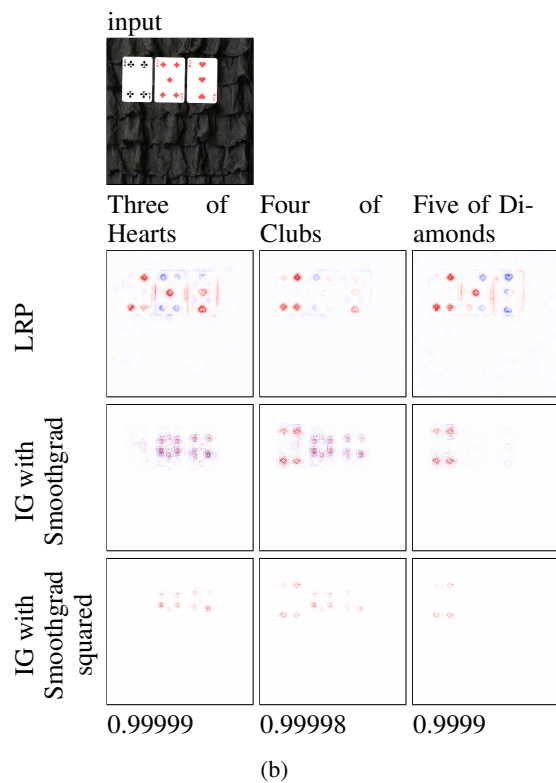
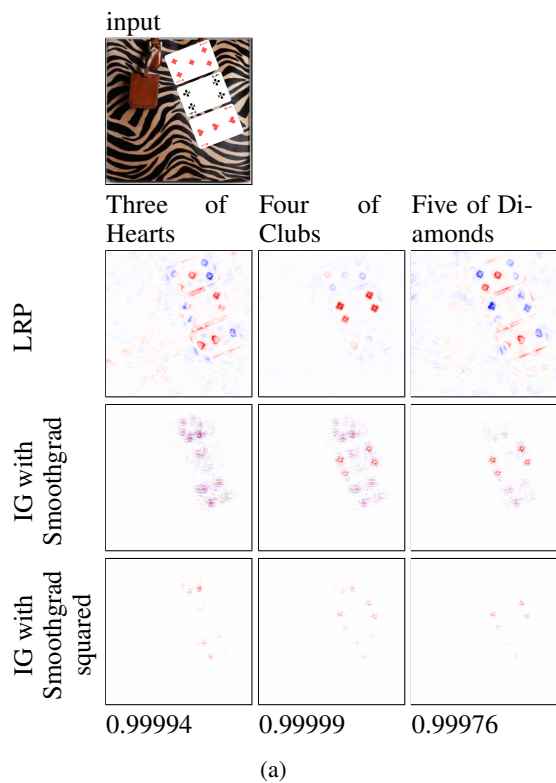


Figure 17: Class-level poker cards predicting concepts with the downstream task classification of Straight

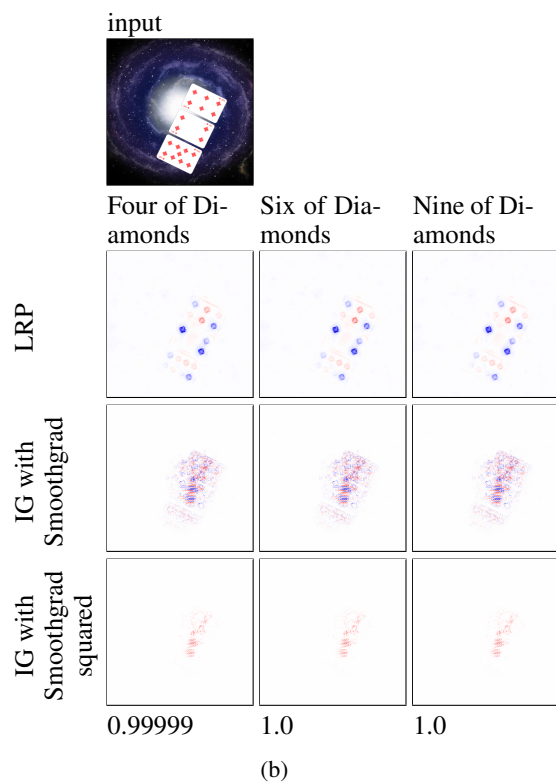
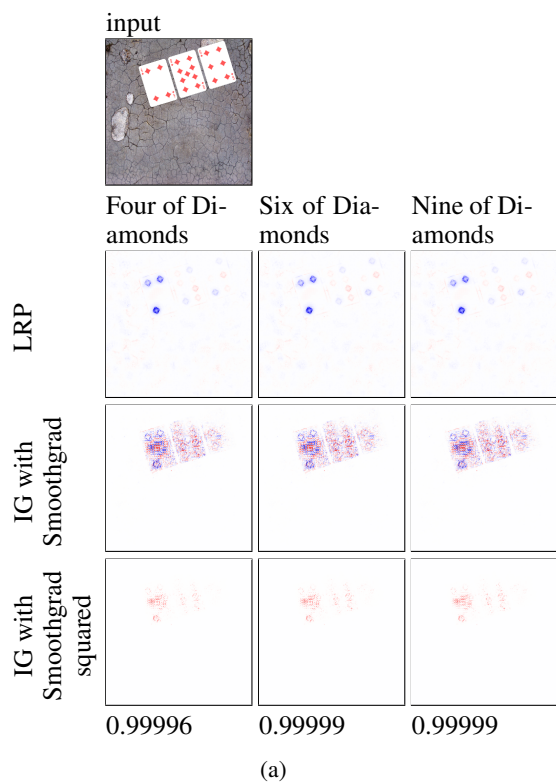


Figure 18: Class-level poker cards predicting concepts with the downstream task classification of Flush

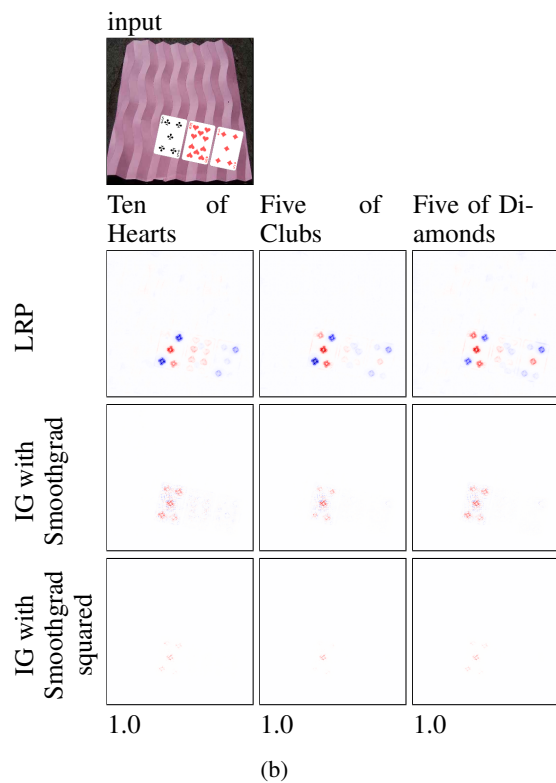
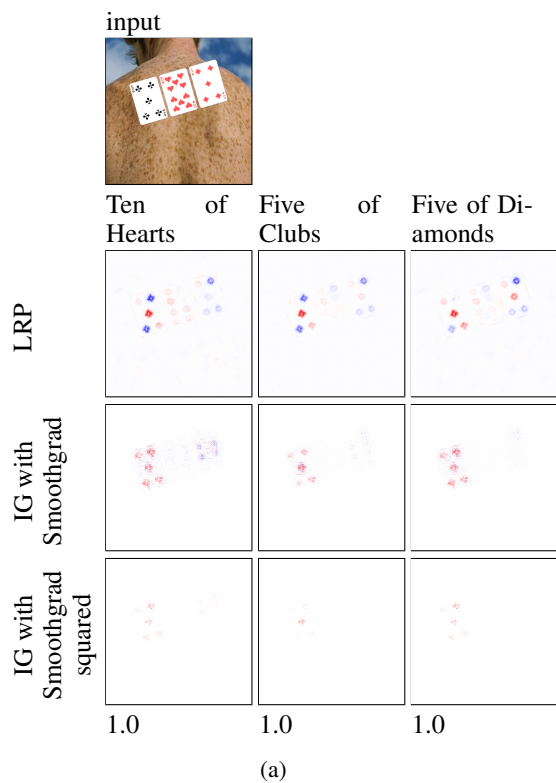


Figure 19: Class-level poker cards predicting concepts with the downstream task classification of Pair

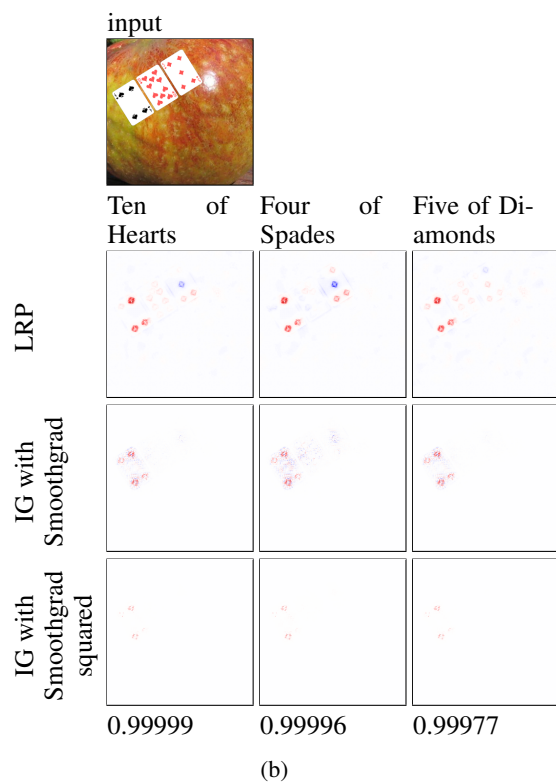
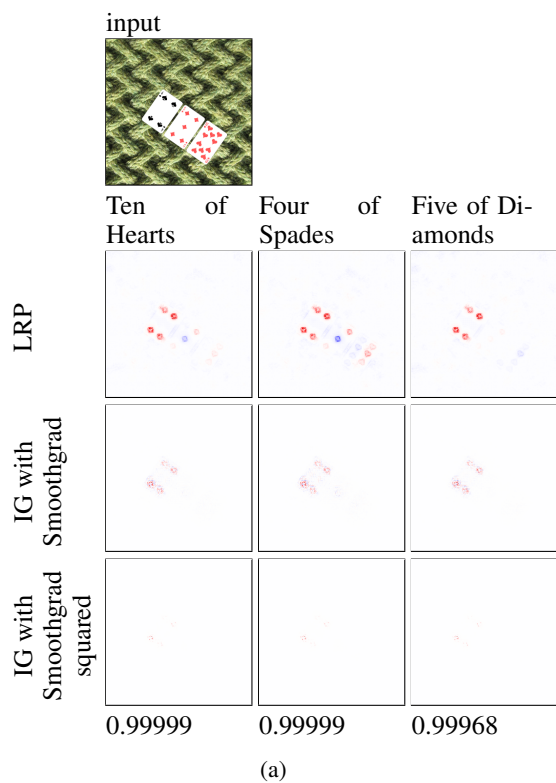


Figure 20: Class-level poker cards predicting concepts with the downstream task classification of High card

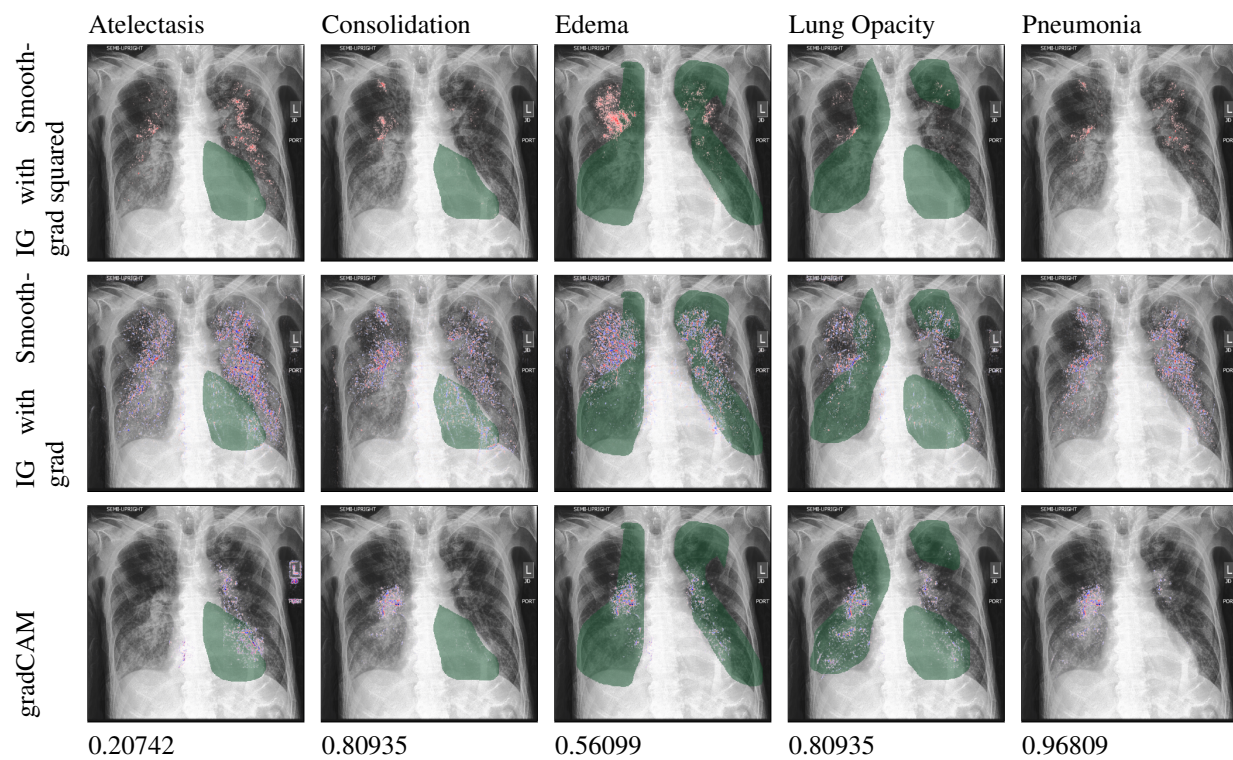


Figure 21: Saliency maps from a instance-level CheXpert trained using the joint CBM method

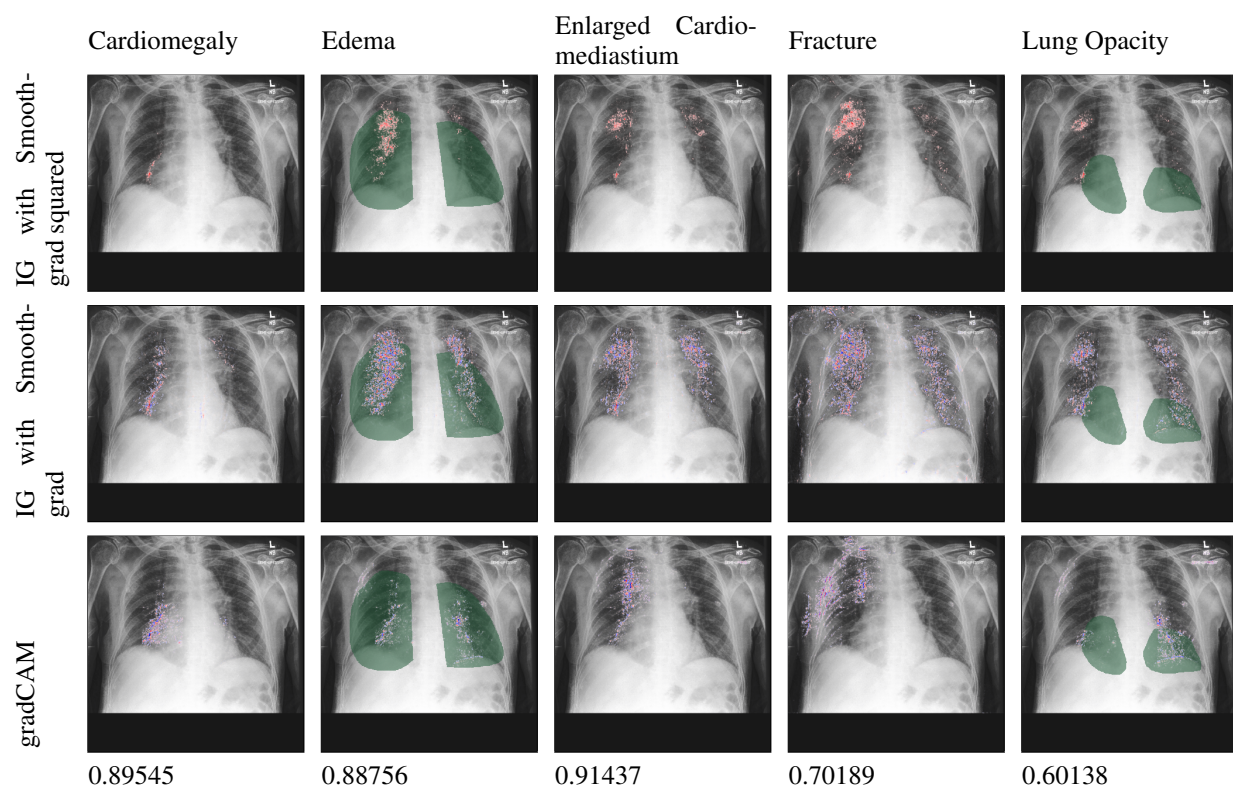


Figure 22: Saliency maps from a instance-level CheXpert trained using the joint CBM method

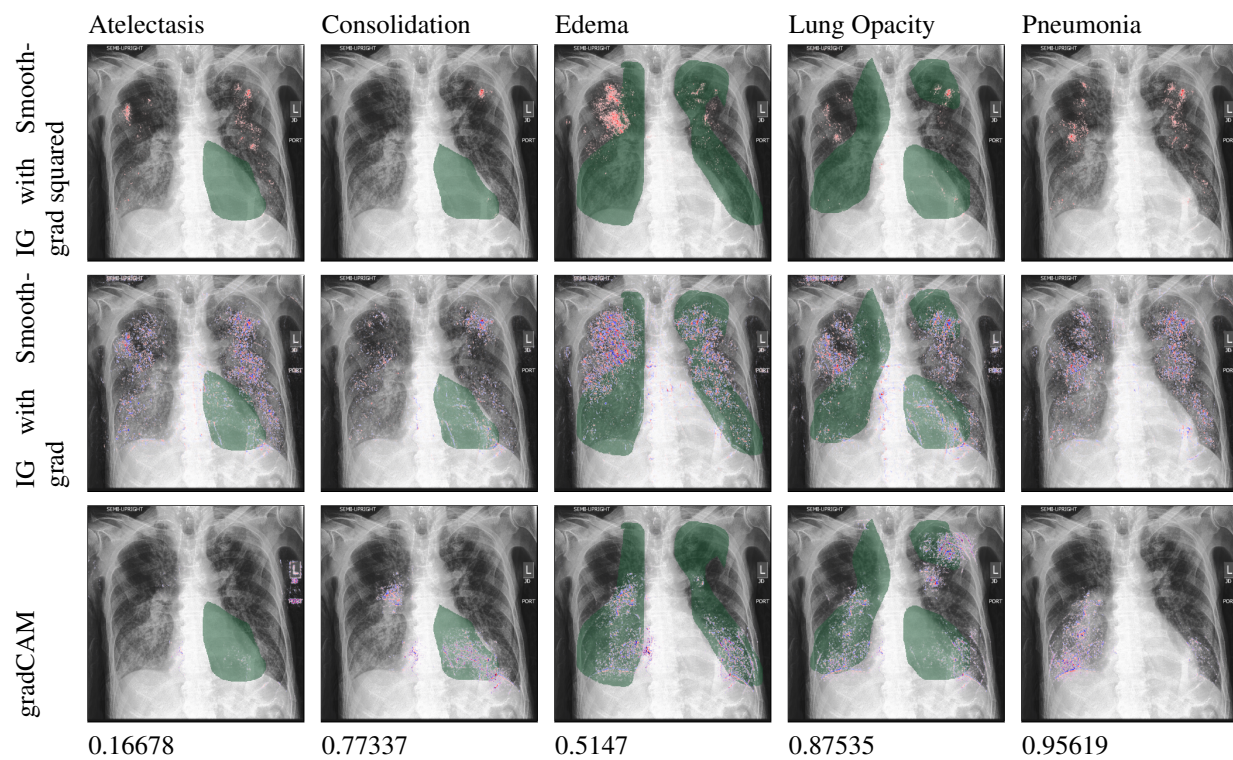


Figure 23: Saliency maps from a instance-level CheXpert trained using the sequential CBM method

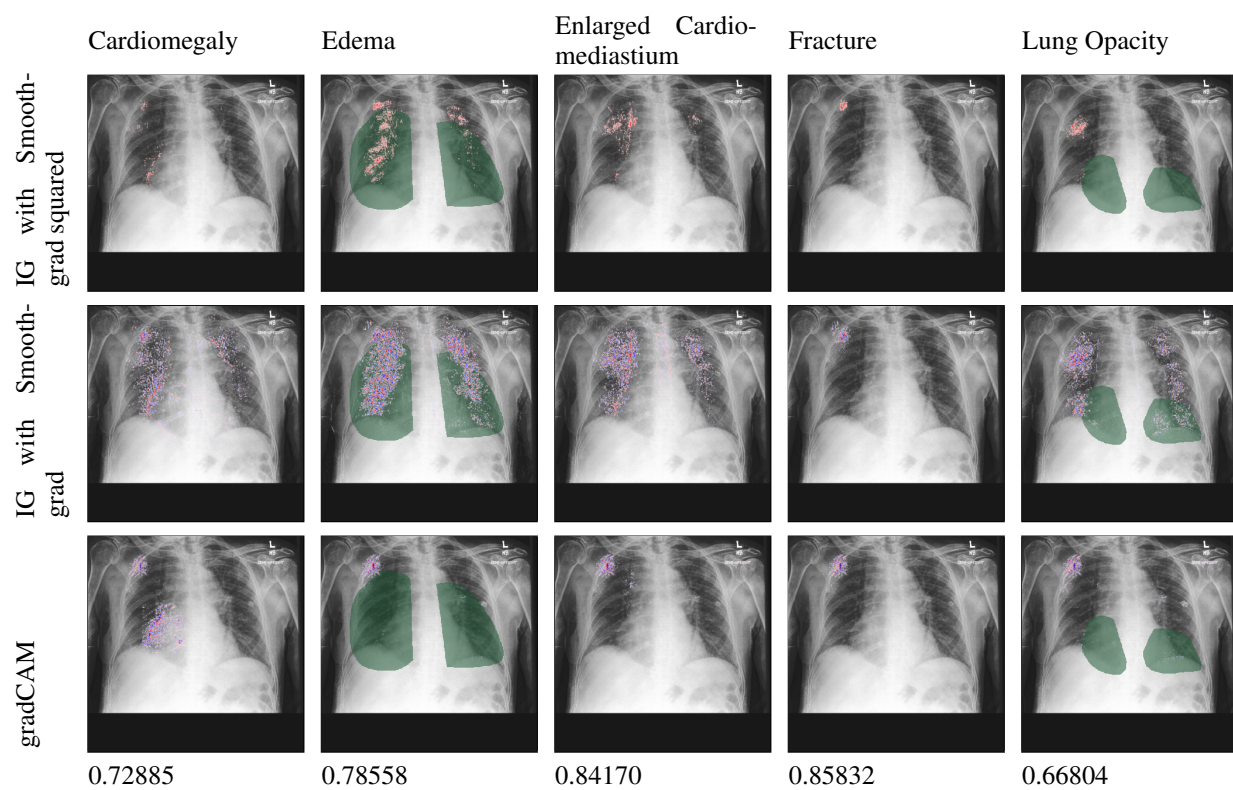


Figure 24: Saliency maps from a instance-level CheXpert trained using the sequential CBM method

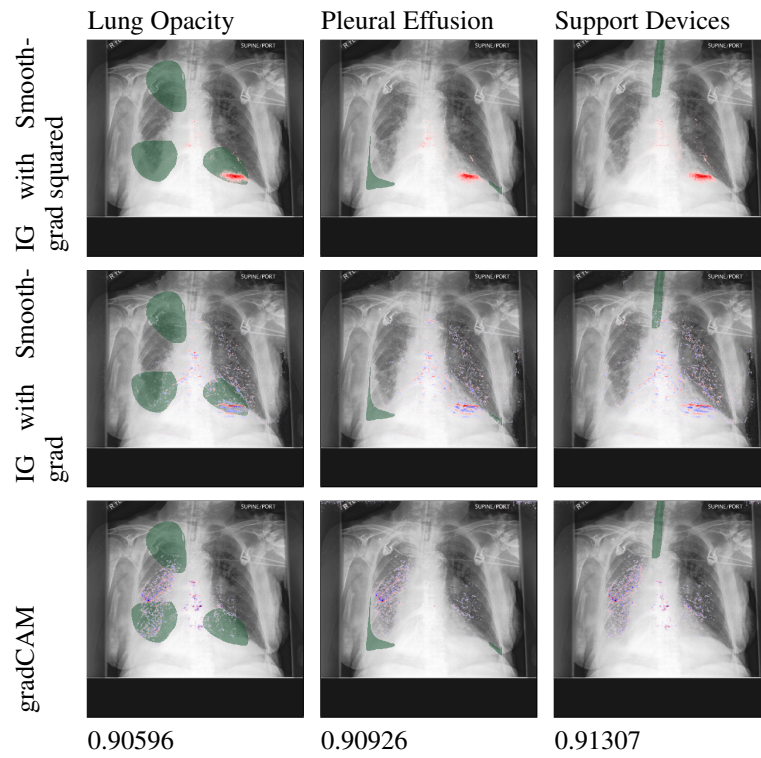


Figure 25: Saliency maps from a class-level CheXpert with three concept present, trained using the sequential CBM method

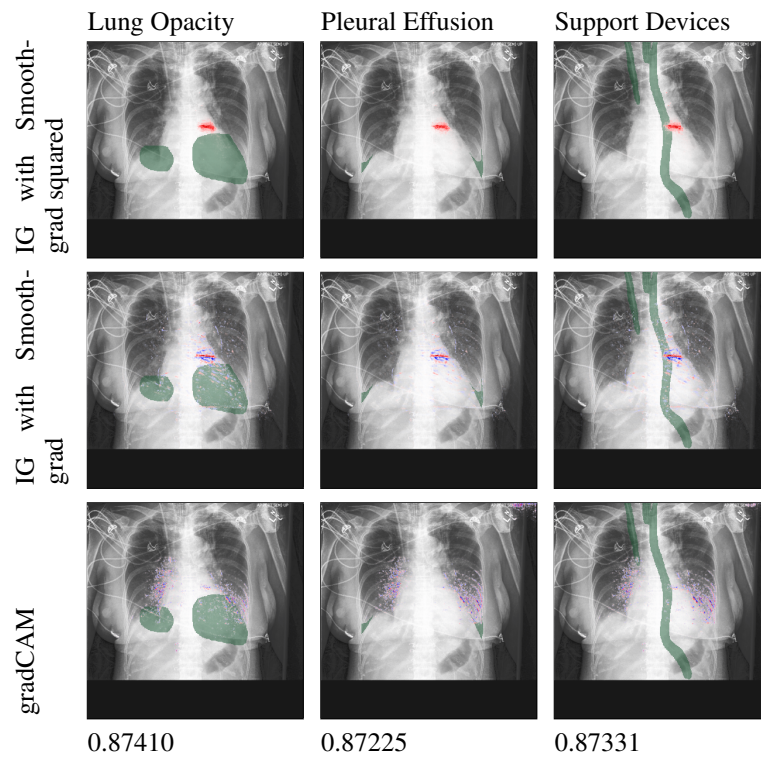


Figure 26: Saliency maps from a class-level CheXpert with three concept present, trained using the sequential CBM method

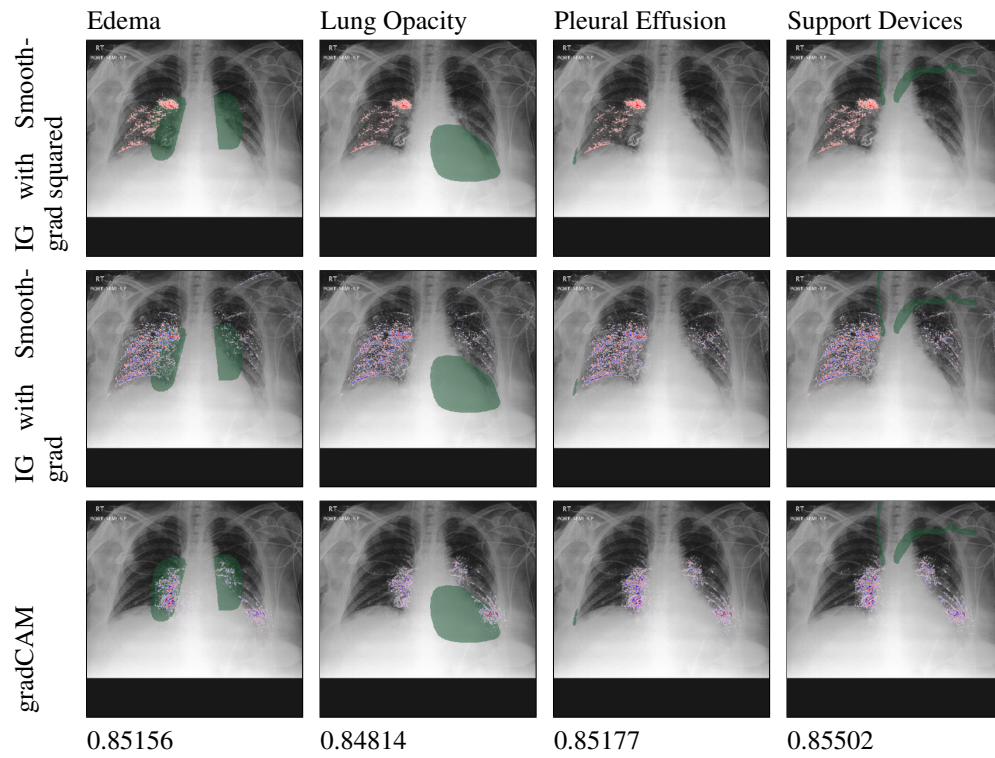


Figure 27: Saliency maps from a class-level CheXpert with four concept present, trained using the sequential CBM method

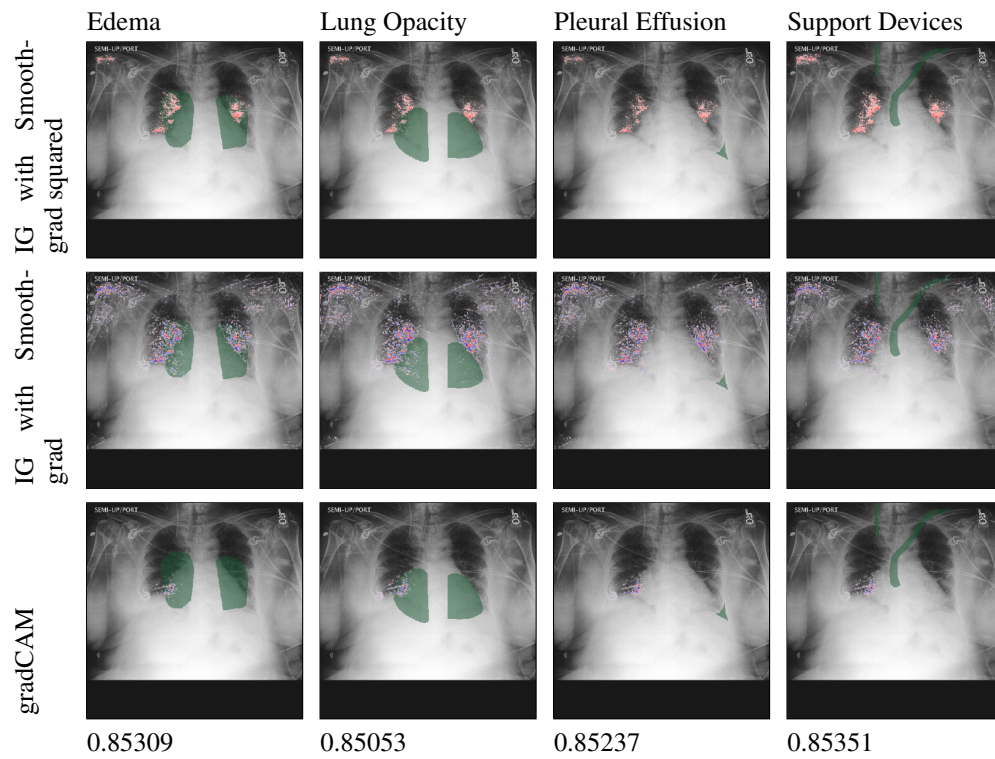


Figure 28: Saliency maps from a class-level CheXpert with four concept present, trained using the sequential CBM method

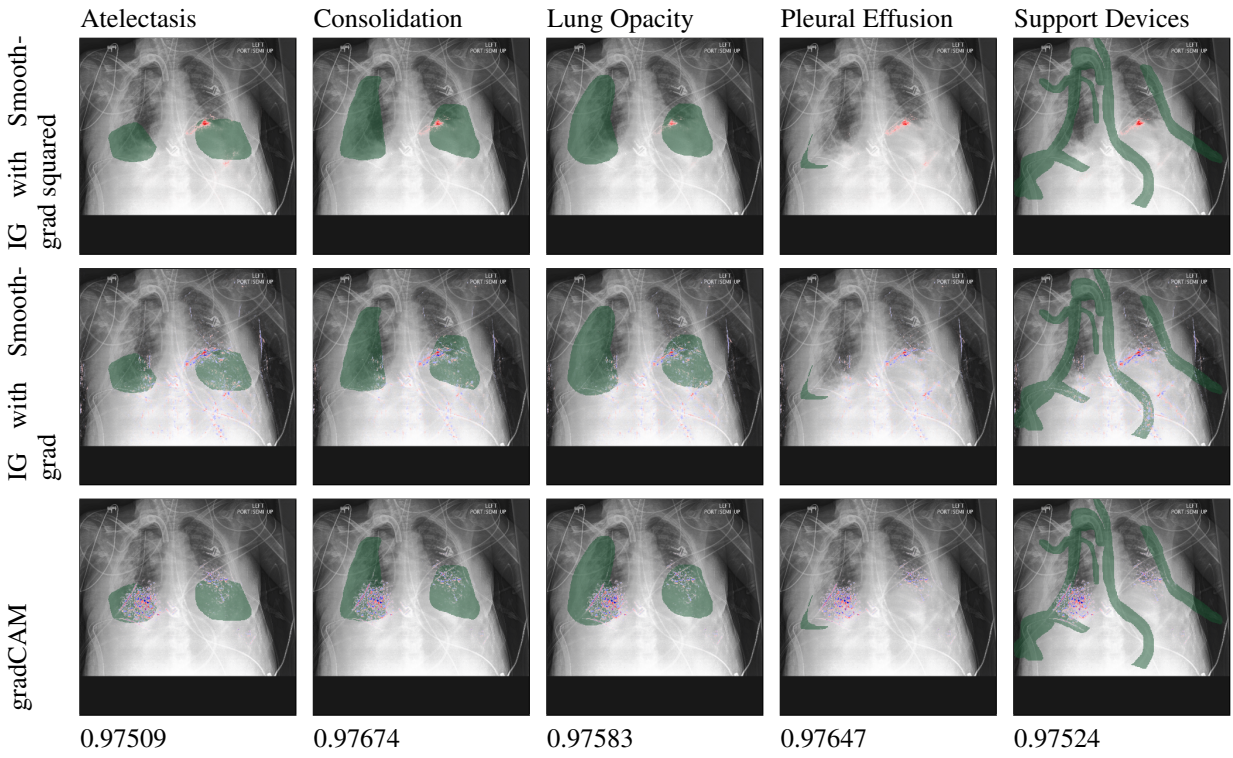


Figure 29: Saliency maps from a class-level CheXpert with five concept present, trained using the sequential CBM method

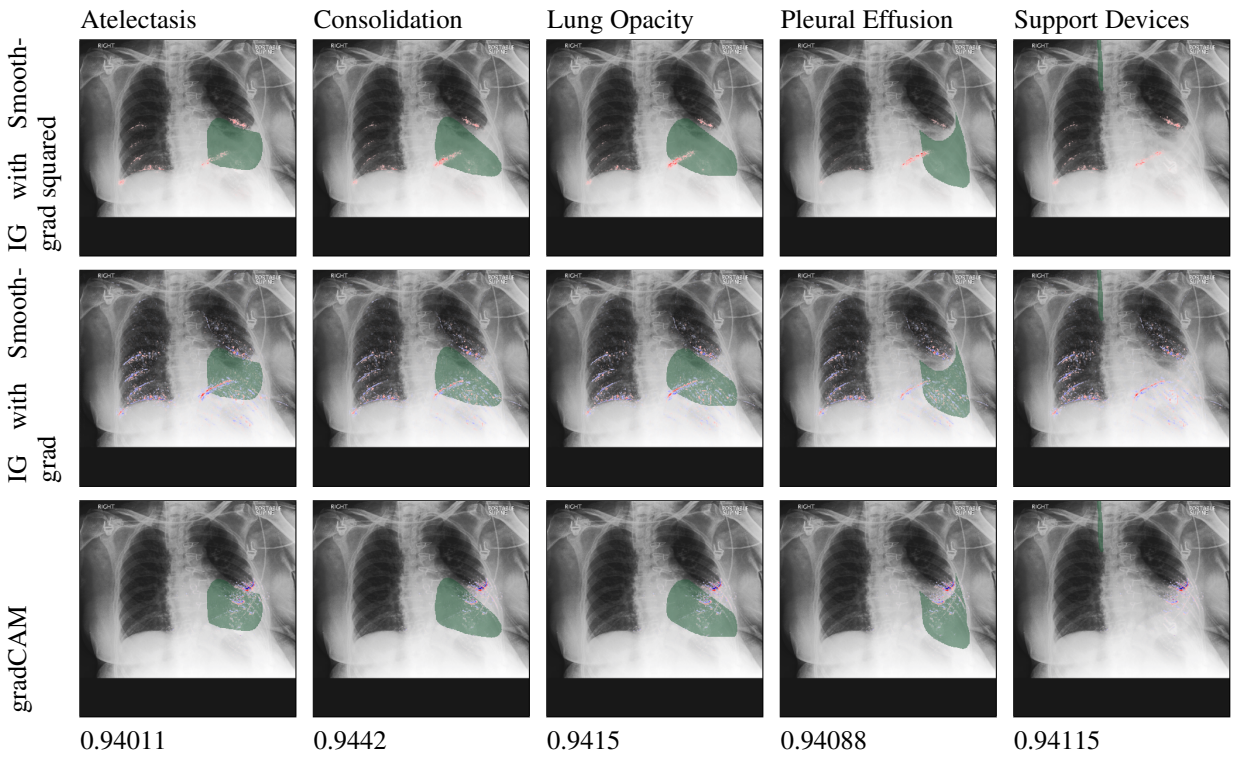


Figure 30: Saliency maps from a class-level CheXpert with five concept present, trained using the sequential CBM method